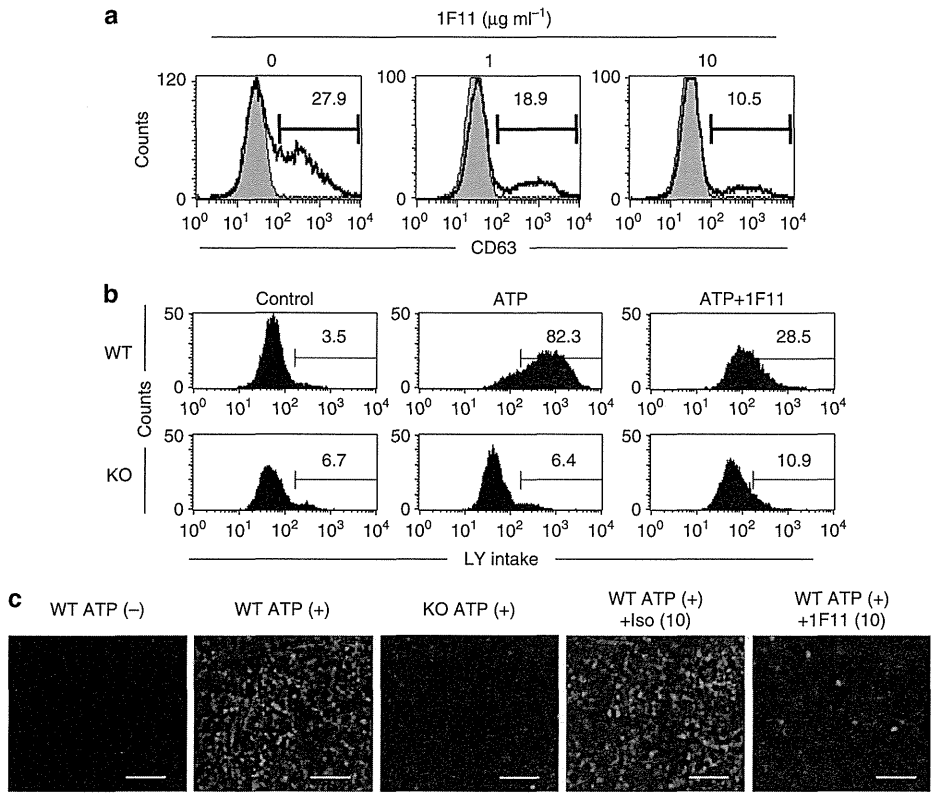

Figure 4 | Inhibition of *in vitro* ATP-mediated MC activation by 1F11 mAb. (**a**) BM-derived MCs, pretreated with various concentrations of 1F11 mAb (0, 1, 10 μg ml^{-1}) for 15 min, were stimulated with 0.5 mM ATP for 30 min. Cells were stained with an anti-CD63 mAb for flow cytometric analysis. Data are representative of three independent experiments. (**b**) BM-derived MCs pretreated with various concentrations of 1F11 mAb or control rat IgG2b (0, 10 μg ml^{-1}) for 15 min were stimulated with 0.5 mM ATP for 30 min in the presence of 1 mg ml^{-1} Lucifer yellow (LY). (**c**) LY uptake was determined by using flow cytometry and fluorescence microscopy. Scale bar, 100 μm. Data are representative of three individual experiments.

ATP stimulation of MCs induced the expression of chemokines, including CCL2, CCL7 and CXCL2 (Fig. 8e–g), and 1F11 mAb treatment or P2X7 deficiency resulted in decreased CCL2 production from MCs activated by ATP but not by IgE plus allergen (Fig. 8g). Furthermore, *Kit*$^{W\text{-}sh/W\text{-}sh}$ mice showed decreased levels of both CCL2 and IL-1β in the colon tissue, but the production levels of these molecules recovered when the mice were reconstituted with wild-type MCs (Supplementary Fig. S10a). As neutrophils express the corresponding chemokine receptors, it is likely that ATP-dependent MC activation induced inflammatory neutrophil infiltration into the colon from the peripheral blood (Supplementary Fig. S10b,c), given the high level of TNFα production by the neutrophils (Supplementary Fig. S10d). These results indicate that ATP-dependent MC activation has key roles in the induction of inflammatory responses (by inducing inflammatory cytokines) and in the exacerbation of inflammatory responses (by inducing LTs and chemokines to recruit TNFα-producing neutrophils to the colon).

Discussion

Here, we showed that MCs have a critical role in the severity of colitis through their interaction with ATP and P2X7 purinoceptors. These interactions not only induce MC-mediated inflammatory responses but also exacerbate them by promoting neutrophil infiltration. Indeed, MC-deficient mice reconstitution with wild-type, but not *P2x7*$^{-/-}$, MCs resulted in neutrophil infiltration and severe inflammatory responses, together with increased production of IL-1β, LTs and CCL2 (Figs 5 and 8, and Supplementary Fig. S10). *Kit*$^{Wsh/Wsh}$ mice spontaneously show elevated levels of neutrophils in their spleens[35]; however, we confirmed that the neutrophil levels were the same as those in the colons of *Kit*$^{+/+}$, *Kit*$^{Wsh/+}$ and *Kit*$^{Wsh/Wsh}$ mice under naïve conditions (Fig. 1h,i). To exclude the possible involvement of other immunological defects in *Kit*$^{Wsh/Wsh}$ mice, such as the involvement of the *Corin* gene, which is associated with type II transmembrane serine protease[35], we further confirmed the amelioration of intestinal inflammation in conditional MC-deficient mice (Fig. 2d–h). These findings strongly suggest that P2X7 on MCs has a pivotal role in the development of murine and human intestinal inflammation.

P2X7 purinoceptors are expressed on T cells, DCs, macrophages and ECs[9–11,25,36]. In a recent study, ATP/P2X7-mediated signalling inhibited the generation and function of regulatory T cells and ATP stimulation led to their conversion into Th17 cells via an IL-6-dependent pathway; thus, the P2X7 antagonist OxATP inhibited colitis[37]. In that study, ATP/P2X7-mediated regulation of regulatory T cells was involved in the chronic phase of intestinal inflammation, which takes about 4 weeks for disease development[37]. Similarly, ATP-mediated DC activation occurs in the chronic phase of intestinal inflammation through the preferential induction of Th17 cells, although whether this is mediated by P2X7 remains to be seen[38]. In contrast, ATP/P2X7-mediated MC activation in our model was important in the development of T-cell-independent acute colitis, which occurs within 1 week. Thus, our study and those of others[37,38] complement each other by reflecting the complicated pathological aspects and kinetics of the acute and chronic phases of intestinal inflammation mediated by ATP and P2X7.

We also found that the expression level of P2X7 receptors differed depending on the tissue and animal species. First, colonic MCs expressed high levels of P2X7, but skin MCs did not

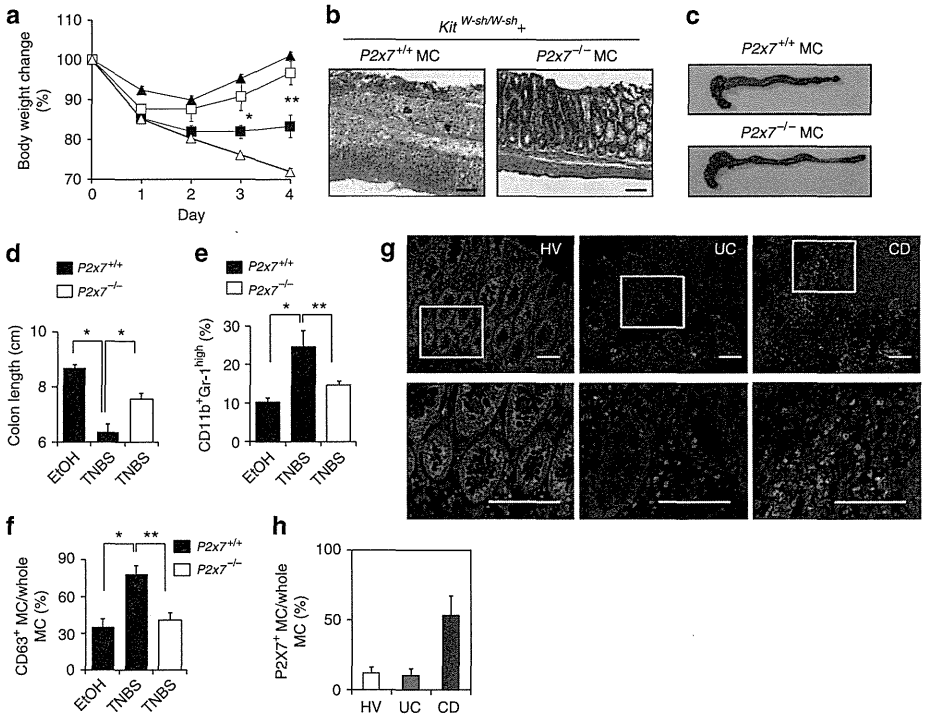

Figure 5 | Inhibitory targeting of P2X7 purinoceptors on MCs leads to amelioration of colonic inflammation. $Kit^{W\text{-}sh/W\text{-}sh}$ MC-deficient mice reconstituted with $P2x7^{+/+}$, $P2x7^{-/-}$ or *caspase-1*$^{-/-}$ BM-derived MCs were applied to a TNBS-induced colitis model. (**a**) Body weight changes were monitored in TNBS-treated $Kit^{W\text{-}sh/W\text{-}sh}$ mice reconstituted with $P2x7^{+/+}$ (closed squares; $n=9$), $P2x7^{-/-}$ (open squares; $n=7$) or *caspase-1*$^{-/-}$ (open triangles; $n=4$). BM-derived MCs were used for TNBS treatment, and $P2x7^{+/+}$ BM-derived MC-reconstituted $Kit^{W\text{-}sh/W\text{-}sh}$ mice receiving EtOH served as controls (closed triangles; $n=3$). $^{*}P=0.0264$ (two-tailed Student's *t*-test), $^{**}P=0.0058$ (two-tailed Student's *t*-test). Data are shown as percentages of baseline weights and are means±s.e.m. (**b**) Representative images of haematoxylin and eosin staining are shown. Scale bars represents 100 μm. (**c**) Representative images of whole colons are shown. (**d**) Colon length was measured 4 days after TNBS administration. Data are shown as means±s.e.m. ($n=3$ for $P2x7^{+/+}$ EtOH, $n=9$ for $P2x7^{+/+}$TNBS, $n=7$ for $P2x7^{-/-}$ TNBS), $^{*}P<0.001$ (two-tailed Student's *t*-test). (**e**) Representative flow cytometric data of infiltrated neutrophils ($CD11b^{+}Gr\text{-}1^{high}$) in the colon from three individual experiments. $^{*}P=0.00741$, $^{**}P=0.0009$ (two-tailed Student's *t*-test). Data are shown as means±s.e.m. (**f**) The percentage of $CD63^{+}$ MCs in all c-kit^{+} FcεRIα^{+} MCs was determined with flow cytometry. Data are shown as means±s.e.m. ($n=3$–9), $^{*}P=0.007$ (Welch's *t*-test), $^{**}P=0.0234$ (Welch's *t*-test). (**g**) Colonic tissue sections from a healthy volunteer (HV) and from UC and CD patients were stained with 4′,6-diamidino-2-phenyl indole (blue), MC tryptase (red) and P2X7 (green). Scale bars, 100 μm. (**h**) Cells expressing both P2X7 and MC tryptase were counted in the fields of the tissue sections (four fields for each section). Data are means±s.e.m. ($n=6$).

(Fig. 3a). Second, in contrast to MCs, some macrophages (for example, microglia and RAW264.7 cells) expressed higher levels of P2X7 than did colonic macrophages (Fig. 3b and data not shown). Third, among the several types of immunocompetent cell in the colon, MCs expressed the highest levels of P2X7 (Fig. 3a,b). Fourth, we found P2X7 expression on human colonic ECs, but not on murine colonic ECs (Figs 3b and 5g). In addition, as reported previously[36], P2X7 expression on ECs was downregulated in the colons of CD patients; instead, CD patients showed increased numbers of $P2X7^{+}$ MCs in their colons (Fig. 5g,h). It is important to note that, like murine MCs, human lung MCs express functional P2X7 (ref. 39). Therefore, although we must recognize the similarities and differences between mouse and human intestinal inflammation and MC distribution, ATP/P2X7-mediated MC activation seems to have a major role in the development of intestinal inflammation.

We found elevated levels of extracellular ATP in the colons of TNBS-treated mice (Fig. 6a). This high ATP concentration was most likely achieved by a combination or cascade of several ATP production pathways (for example, cell injury or lysis[7], pattern recognition receptor-mediated activation of monocytes[40] and commensal bacteria[38]). In our tissue culture system, we detected elevated release of ATP (40 μM) in the inflamed colon compared with the control (Fig. 6); however, at least 100 μM ATP was required for MC activation *in vitro* in the single cell culture system (Fig. 7b). This disparity likely reflects the differences in the culture conditions. Unlike in the single cell culture system, the concentration of secreted ATP in the tissue culture system could have been diluted in the culture medium, or ATP could have been consumed rapidly by activated inflammatory cells in the tissue. Alternatively, a lack of commensal bacteria-derived ATP in the tissue culture system as a result of the inclusion of antibiotics may have reduced the ATP level. Another possibility is that the abundant endogenous ATP-degrading enzymes (for example, CD39) in the colon tissue may have degraded some of the ATP. In support of this idea, a suppressive role for CD39 in intestinal inflammation has been reported[41].

We found that ADP-reactive P2Y1 and P2Y12 receptors were expressed on colonic MCs (Fig. 7c), but inhibition or knockdown of these receptors did not suppress the CD63 expression (Fig. 7d,e; Supplementary Fig. S8a). In previous studies, stimulation of MCs with ADP (0.05–50 μM) has led to calcium influx via the P2Y1- but not the P2Y12-mediated pathway[42], whereas our results indicate that CD63 expression required a higher concentration of ADP and was not suppressed by a P2Y1 inhibitor (Fig. 7b,d). This finding indicates that P2Y purinoceptors are not involved in the induction of $CD63^{+}$-activated MCs that is mediated by high concentrations of ADP. However, we found that adenylate kinase and ATP synthase converted ADP back to ATP, which subsequently induced P2X7

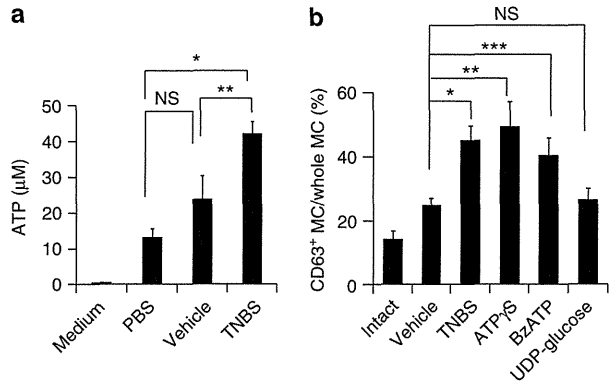

Figure 6 | Enhanced ATP production in intestinal inflammation and MC activation induced by non-hydrolyzable ATP. (**a**) The concentration of ATP released from the colon tissue of mice receiving intrarectally administered phosphate-buffered saline, vehicle or TNBS was measured. Data are shown as means±s.e.m. ($n=3$–7). *$P=0.0004$, **$P=0.0447$ (two-tailed Student's *t*-test). (**b**) CD63 expression of colonic MCs was measured with flow cytometry after intrarectal administration of vehicle ($n=14$), TNBS ($n=5$), non-hydrolyzable ATP (adenosine 5′-O-(3-thio) triphosphate (ATPγS); $n=9$ or O-(4-benzoyl)benzoyl adenosine 5′-triphosphate (BzATP); $n=10$) or UDP-glucose ($n=6$), or in intact mice ($n=7$). Data are shown as means±s.e.m. *$P=0.0002$ (two-tailed Student's *t*-test), **$P=0.0135$ (Welch's *t*-test) and ***$P=0.0238$ (Welch's *t*-test). NS, not significant.

purinoceptor-dependent MC activation. A similar conversion of ADP to ATP has been reported for endothelial cells[27]. Among adenylate kinases, AK2 was highly expressed on MCs and had a pivotal role in the conversion of ADP to ATP (Supplementary Fig. S9a,b). As another P2Y ligand (UTP) did not induce MC activation (Fig. 7b), our findings suggest that ADP could be converted into ATP by AK2 and ATP synthase, and that this ATP subsequently activates MCs through P2X7 purinoceptors. In addition, colonic MCs do not express ecto-5′-nucleotidase (CD73), an enzyme that degrades ADP into adenosine, which has anti-inflammatory effects in intestinal inflammation[43]. Therefore, our study indicates that MCs express CD39, adenylate kinases and ATP synthase, but not CD73, to preferentially convert ADP to ATP for the exacerbation of inflammatory responses through P2X7 purinoceptors.

Here, we showed that colitis aggravated by P2X7-mediated activation of MCs was independent of the inflammasome pathway, and that P2X7-mediated activation of MCs promoted TNFα production by effector cells to further promote intestinal inflammation[44]. Our findings also suggest that MCs exacerbate inflammation by recruiting neutrophils to produce abundant TNFα, but less IL-10 than is produced by other cells (for example, eosinophils, DCs and macrophages; Supplementary Fig. S10d). This neutrophil recruitment was mediated by the production of IL-1β, LTs and chemokines, which are potential targets for the treatment of colitis. Mice with experimentally induced colitis that lack CXCR2 or 5-LO (a key enzyme for converting arachidonic acid to LTs), as well as mice treated with inhibitors of CCR2, CXCR2 or 5-LO, show reduced inflammation and less neutrophil recruitment in their colons[33,45,46]. Moreover, given that ATP promotes neutrophil migration[47], it is possible that P2X7-dependent LT and chemokine production, as well as ATP generation via AK2 and ATP synthase from MCs, could amplify neutrophil infiltration of the colon. These data collectively indicate that MCs are key factors in the induction of intestinal inflammation and also recruit neutrophils to heighten inflammatory responses. P2X7-dependent MC activation could, therefore, be a target for the treatment of intestinal inflammation.

Methods

Mice and human samples. Female C57BL/6 mice were purchased from CLEA Japan. Rag1$^{-/-}$ and P2x7$^{-/-}$ mice were obtained from Jackson Laboratory (Bar Harbour, ME, USA). MC-deficient *Kit*$^{W\text{-}sh/W\text{-}sh}$ mice were obtained from Dr H. Suto (Atopy Research Center, Juntendo University, Japan). For the conditional MC-deficient analysis, Mas-TRECK tg mice were injected intraperitoneally with 250 ng of diphtheria toxin for 5 consecutive days and then with 150 ng every other day[18]. *Caspase-1*$^{-/-}$ mice were backcrossed with C57BL/6 mice; F5 mice were used for this experiment[48]. All mice were maintained under specific-pathogen-free conditions at the Experimental Animal Facility of the Institute of Medical Science, the University of Tokyo. All experiments were approved by the Animal Care and Use Committee of the University of Tokyo.

MC reconstitution was performed as described previously[49]. Briefly, BM-derived MCs were obtained from *P2x7*$^{+/+}$, *P2x7*$^{-/-}$ or *caspase-1*$^{-/-}$ mice as described previously[22]. BM-derived MCs (5×10^6) were intravenously transferred to *Kit*$^{W\text{-}sh/W\text{-}sh}$ mice at two time points (0 and 14 days). The reconstituted mice were used 3 months after the last transfer.

Colon specimens from UC and CD patients and healthy volunteers were obtained by endoscopic biopsy at Osaka University Hospital. All subjects provided written informed consent, and the study protocol was approved by the Ethics Committee of Osaka University Graduate School of Medicine (no. 08243) and the Institute of Medical Science, The University of Tokyo (no. 20-67-0331).

Experimental colitis. For TNBS-induced colitis, anaesthetized mice (18–22 g) were sensitized with 2.5% TNBS (Sigma-Aldrich) together with acetone and olive oil[50]. After 1 week, after a 3-h fast, the mice were given 100 μl of 2.5% TNBS in 50% ethanol via a flexible feeding tube that maintained their heads in a vertical position for 10 min. The control group received only 50% ethanol. Weight changes were recorded daily, and tissues were collected for histological analysis and isolation of mononuclear cells from the colonic lamina propria. For mAb treatment, mice were injected intraperitoneally with 0.5 mg of mAb (1F11 or an isotype control) 1 day before being given TNBS/EtOH intrarectally. mAb administration was continued for 3 days. For P2Y12 inhibition with clopidogrel sulphate, (Wako, Osaka, Japan), mice received clopidogrel (0.5 mg ml^{-1}) in their drinking water from 3 days before intrarectal administration of TNBS/EtOH until the end of the study[50]. For DSS-induced colitis, mice were given 3.5% DSS (Wako, for C57BL/6) or 2.5% DSS (MP Biomedicals, Illkirch, France, for Mas-TRECK tg mice) in their drinking water for 5 days and their body weights were monitored daily[50]. In some experiments, non-hydrolysable ATP (adenosine 5′-*O*-(3-thio) triphosphate and *O*-(4-benzoyl)benzoyl adenosine 5′-triphosphate) or UDP-glucose (0.25 mg in 50% EtOH) was intrarectally administered and the effects were analysed 2 days later.

***In vitro* MC stimulation and inhibition.** BM-derived MCs (2.5×10^5) were cultured with various concentrations of adenosine, ADP, ATP, UTP or anti-DNP-IgE with DNP-human serum albumin. Adenosine-3-phosphate 5-phosphosulfate (0.25 mM), carbenoxolone (10 μM), flufenamic acid (100 μM), pyridoxal-phosphate-6-azophenyl-2′,4′-disulfonate (100 μM), 4,4′-diisothiocyanatostilbene-2,2′-disulfonic acid disodium salt hydrate (100 μM), OxATP (0.5 mM), AD2P5 (1 mM), oligo (10 or 100 μM) or UDP (100 μM) was added to the cells for the inhibition assay[27,28,40,51]. All reagents were purchased from Sigma-Aldrich (St Louis, MO, USA, purity was ≥95%). 5-LO (BD Pharmingen, Franklin Lakes, NJ, USA) was stained after permeabilization with 0.2% Triton-X100 for 10 min; nuclei were stained with 4′,6-diamidino-2-phenyl indole.

Cell preparation and flow cytometry. ECs and lamina propria mononuclear cells were isolated from the colon, as described previously[52]. For flow cytometric analysis, cells were incubated with 5 μg ml^{-1} of an anti-CD16/32 antibody (10 μg ml^{-1}, Fc block, BD Pharmingen) for 5 min and stained for 30 min at 4 °C with fluorescence-labeled Abs specific for c-kit (0.2 μg ml^{-1}), Gr-1 (0.4 μg ml^{-1}), CD4 (1 μg ml^{-1}), CD11b (0.2 μg ml^{-1}), CD11c (0.4 μg ml^{-1}), CD39 (0.4 μg ml^{-1}), CD45 (0.4 μg ml^{-1}), IgA (10 μg ml^{-1}), B220 (0.4 μg ml^{-1}; BD Pharmingen), CCR3 (2 μg ml^{-1}), CXCR2 (4 μg ml^{-1}; R&D Systems, Minneapolis, MN, USA), FcεRIα (0.4 μg ml^{-1}), CD73 (0.4 μg ml^{-1}), TLR2 (10 μg ml^{-1}; eBioscience, San Diego, CA, USA), F4/80 (20 μg ml^{-1}), CCR2 (10 μg ml^{-1}), P2X7 (Hano43; 2 μg ml^{-1},Serotec, UK) or CCR1 (10 μg ml^{-1}, Abnova, Taiwan). Flow cytometric analysis and cell sorting were performed by using FACSCalibur and FACSAria (BD Biosciences, Franklin Lakes, NJ, USA), respectively. Sorted cells were stained with May-Giemsa stain in some experiments. Colonic MCs and BM-derived MCs were prepared as described elsewhere[22].

Establishment of an anti-P2X7 mAb (1F11) and an anti-CD63 mAb. The procedure used to establish MC-specific mAbs is shown as a flowchart in Supplementary Figure S3. Briefly, c-kit$^+$ FcεRIα$^+$ MCs were obtained as described previously[22] from the colons of mice that exhibited allergic diarrhoea. Purified colonic MCs (10^6 cells) were injected into the footpads of Sprague Dawley rats seven times, as described previously[53]. Lymphocytes were isolated from the spleen and inguinal lymph nodes and fused with P3X63-AG8.653 myeloma cells (CRL-1580; American Type Culture Collection, Manassas, VA, USA). The reactivity of each hybridoma to the colonic MCs was examined by means of flow cytometry. To identify antigens

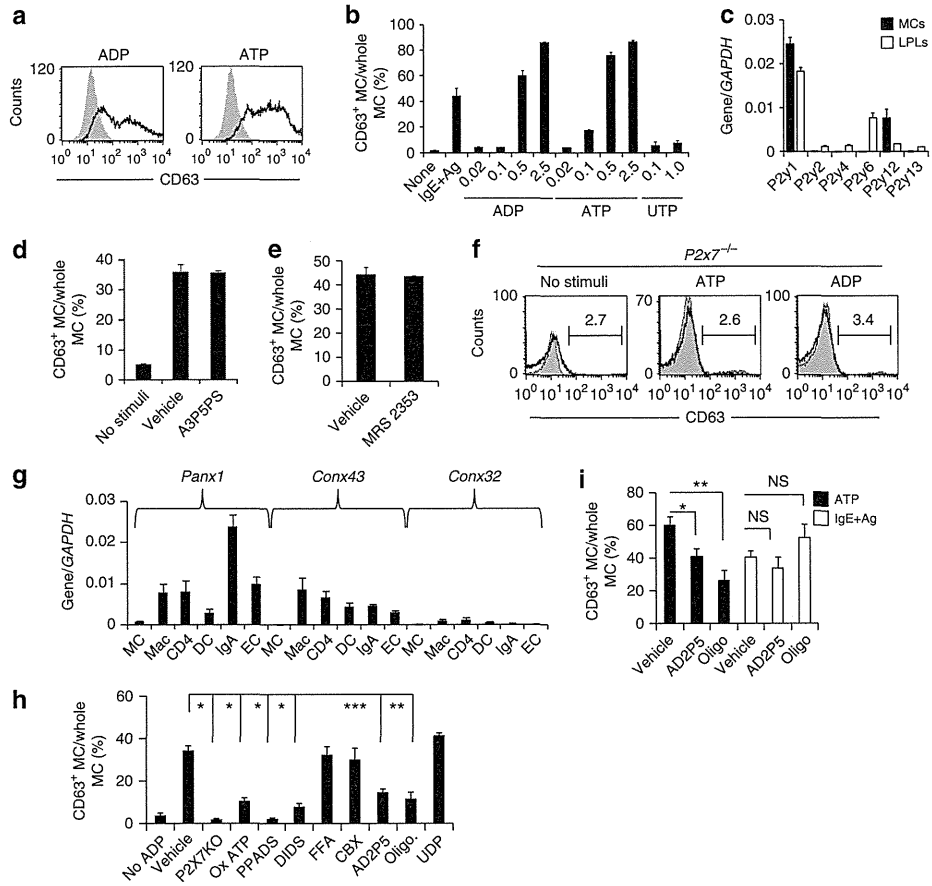

Figure 7 | The ecto-adenylate kinase pathway mediates ADP-dependent MC activation through P2X7 purinoceptors. (**a**) BM-derived MCs treated with ADP or ATP at 0.5 mM for 30 min and examined for CD63 expression. (**b**) BM-derived MCs treated with IgE plus relevant allergen or various concentrations of ADP, ATP or UTP for the analysis of CD63 expression. Data are representative of four experiments. (**c**) Expression of mRNA encoding each P2Y receptor in colonic lamina propria lymphocytes (LPLs) and MCs was analysed by quantitative reverse transcription (RT)-PCR ($n=3$). (**d**,**e**) BM-derived MCs pre-treated with 0.25 mM P2Y1 inhibitor (adenosine-3-phosphate 5-phosphosulfate (A3P5PS)) (**d**) or 0.01 mM P2Y12 inhibitor (MRS2353) (**e**), stimulated with ADP and examined for CD63 expression ($n=3$). (**f**) BM-derived MCs from *P2x7*$^{-/-}$ mice stimulated with ATP or ADP; CD63 expression was determined with flow cytometry. Data are representative of four experiments. (**g**) Expression of pannexin-1 (Panx1), connexin-43 (Conx43) and Conx32 on colonic MCs, macrophages (Mac), CD4$^+$ T cells (CD4), DCs, IgA$^+$ cells (IgA) and ECs was measured by quantitative RT-PCR ($n=4$). (**h**) BM-derived MCs were pretreated with inhibitors of P2X receptors [OxATP, 0.5 mM; pyridoxal-phosphate-6-azophenyl-2′,4′-disulfonate (PPADS); 4,4′-diisothiocyanatostilbene-2,2′-disulfonic acid (DIDS)], connexins [flufenamic acid (FFA)], Panx-1 [carbenoxolone (CBX)], ecto-adenylate kinase [diadenosine pentaphosphate (AD2P5)], ATP synthase (oligomycin) or nucleoside diphosphokinase (UDP) and subsequently stimulated with 0.25 mM ADP. CD63 expression was determined with flow cytometry. ($n=3$) $^*P<0.01$, $^{**}P<0.05$ (two-tailed Student's *t*-test). All data are shown as means±s.e.m. (**i**) BM-derived MCs were treated with AD2P5, oligomycin or UDP and stimulated with 0.5 mM ATP or IgE plus allergen. CD63 expression was determined with flow cytometry ($n=5$). $^*P<0.0001$ (two-tailed Student's *t*-test), $^{**}P=0.0008$ (two-tailed Student's *t*-test) and $^{***}P=0.0008$ (Welch's *t*-test). NS, not significant.

recognized by the mAbs, immunoprecipitation was performed with the mAbs, followed by Liquid chromatography–mass spectrometry analysis, as described previously[53]. Antigen specificity was confirmed by transfecting CHO cells with plasmids that encoded the murine P2X7 receptor and CD63.

Measurements of membrane permeability and inflammatory mediators. To assess membrane permeability, BM-derived MCs were washed twice with phosphate-buffered saline (PBS) and incubated with 1 mg ml^{-1} Lucifer yellow (Sigma-Aldrich) containing 250 μM sulfinpyrazone (Sigma-Aldrich). The MCs were then stimulated with 0.5 mM ATP (Sigma-Aldrich) for 15 min, as described elsewhere[12]. In the inhibition assay, 1 or 10 μg ml^{-1} of 1F11 mAb or the control antibody (Rat IgG2b) was added before ATP stimulation. The fluorescence signal of Lucifer yellow was determined by using fluorescence microscopy (BZ9000, Keyence, Osaka, Japan) and flow cytometry.

To measure the production of cytokines, chemokines and LTs from MCs, BM-derived MCs (2.5×10^5) were stimulated with 2.5 mM ATP for 30 min, after which the supernatants were collected. Chemokine and cytokine production was detected with an inflammatory cytokine kit (BD Pharmingen). For IL-1β measurement, BM-derived MCs from wild-type, *P2x7*$^{-/-}$ and *caspase-1* $^{-/-}$ mice were stimulated with 0.1 μg ml^{-1} of LPS for 4 h, followed by ADP or ATP stimulation. LT C4/D4/E4 production was detected by use of an enzyme-linked immunosorbent assay (GE Healthcare Bio-Science, NJ, USA). For ATP, cytokine and chemokine measurements from the colon tissue, the colon tissues were isolated from mice 2 days after intrarectal administration of TNBS. Released ATP was measured by culturing colon tissues at 100 mg of tissue per 100 μl of RPMI1640 medium for 3 h and using a luminescence ATP detection system (PerkinElmer, Norwalk, CT, USA).

Immunoprecipitation and western blotting. Cell lysates obtained from BM-derived MCs or CHO transfectants (mouse P2X7 variants a, c and d and flag-mP2X7s, cloned from C57BL/6 mice) were analysed by western blotting and immunoprecipitation with 1F11 mAb or the control Ab. Membranes were probed with an anti-flag and a polyclonal rabbit anti-P2X7 antibody (Sigma-Aldrich).

Histology. Colonic tissues were fixed in 4% paraformaldehyde and embedded in paraffin. Tissue sections (5 μm) were stained with haematoxylin and eosin solution, as described previously[22]. For the detection of MCs and P2X7

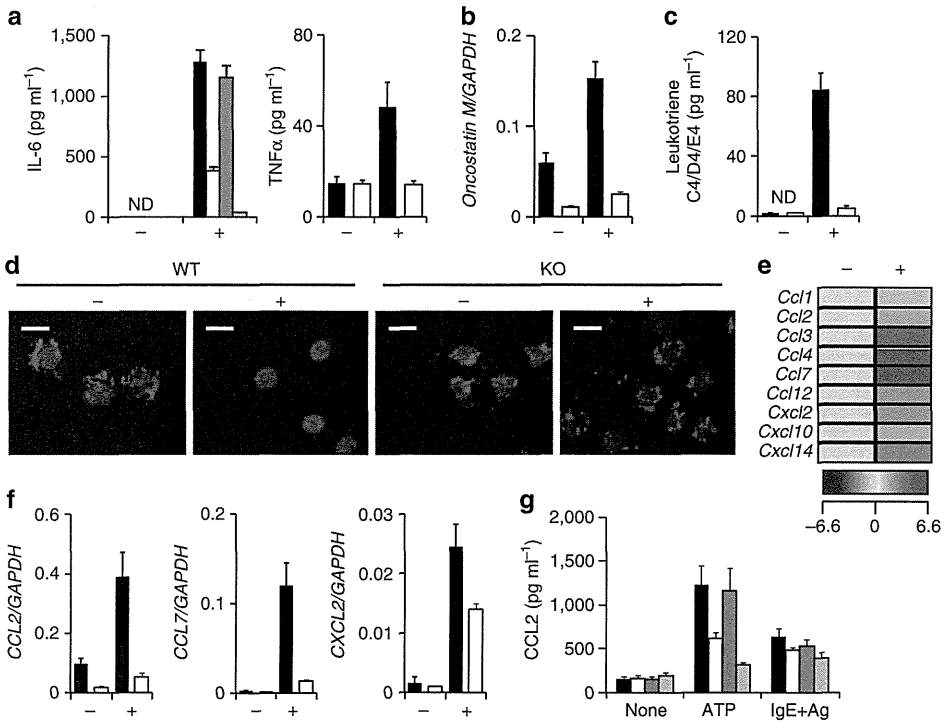

Figure 8 | Critical role of the intestinal MC-associated ATP-P2X7 purinoceptor pathway for induction of neutrophil infiltration. *P2x7*$^{+/+}$ and *P2x7*$^{-/-}$ BM-derived MCs were treated with 0.25 mM ATP (+) or left untreated (−). (**a**) Production of IL-6 (left panel; isotype mAb-treated MC, closed column; 1F11 mAb-treated MC, open column; *P2x7*$^{+/+}$, grey column; and *P2x7*$^{-/-}$, beige column) and TNFα (right panel) in culture supernatant (*P2x7*$^{+/+}$, closed column; *P2x7*$^{-/-}$, open column) was determined after 24 h stimulation. ND, not detected. Data are shown as means±s.e.m. ($n=3$). (**b**) Oncostatin M mRNA expression was measured 30 min after stimulation of *P2x7*$^{+/+}$ (closed column) and *P2x7*$^{-/-}$ (open column) MCs with ATP. Data are shown as means±s.e.m. ($n=3$). (**c**) LT C4/D4/E4 production from ATP-stimulated (+) or -unstimulated (−) *P2x7*$^{+/+}$ (closed column) or *P2x7*$^{-/-}$ BM-derived MCs (open column) in culture supernatants was measured by using enzyme-linked immunosorbent assay (ELISA). Data are shown as means±s.e.m. ($n=3$). ND, not detected. (**d**) *P2x7*$^{+/+}$ and *P2x7*$^{-/-}$ BM-derived MCs were stimulated with 0.5 mM ATP. Cells were fixed and stained with an anti-5LO antibody (red) and 4′,6-diamidino-2-phenyl indole (blue). Scale bar, 10 μm. Data are representative of two experiments. (**e**) Representative data of a chemokine gene array are shown. Increased levels of each chemokine are shown as a heat map. (**f**) mRNA expression of CCL2 (left), CCL7 (middle) and CXCL2 (right) was measured by using quantitative reverse transcription–PCR. Data are shown as means±s.e.m. ($n=3$). (**g**) CCL2 production was enumerated by using ELISA 24 h after stimulation of BM-derived MCs with ATP or IgE plus antigen (IgE+Ag). Isotype mAb-treated MC, closed column; 1F11 mAb-treated MC, open column; *P2x7*$^{+/+}$ MC, grey column; and *P2x7*$^{-/-}$ MC, beige column). Data are shown as means±s.e.m. ($n=3$).

expression in human specimens, colonic tissue sections were stained with antibodies for MC tryptase and P2X7 purinoceptors (Alomone Laboratories, Jerusalem, Israel).

shRNA plasmid construction and lentiviral transduction. For the construction of shRNA expression lentivirus vector plasmids, a series of oligonucleotide pairs were synthesized, as listed below. Each oligo pair was annealed and cloned into pmU6[54]. Each mU6-shRNA cassette was then subcloned into the ΔU3 sequence of the 3′-LTR of the lentivirus vector plasmid pLCG to generate pLCG-shCD63 (sense: 5′-TTTGATTCTTGCTGCATCAACATAGCTTCCTGTCACTATGTTGATGCAG CAAGAATCTTTTTTG-3′, antisense: 5′-AATTCAAAAAAGATTCTTGCTGCA TCAACATAGTGACAGGAAGCTATGTTGATGCAGCAAGAAT-3′), pLCG-shP2Y12 (sense: 5′-TTTGATCTACTAATGATTCTAACTGCTTCCTGTCACAGTTAGAAT CATTAGTAGATCTTTTTTG-3′, antisense: 5′-AATTCAAAAAAGATCTACTAA TGATTCTAACTGTGACAGGAAGCAGTTAGAATCATTAGTAGAT-3′) and pLCG-shAK1 (sense: 5′-TTTGCGAGAAGATTGTACAGAAATGCTTCCTGTCA CATTTCTGTACAATCTTCTCGCTTTTTTG-3′, antisense: 5′-AATTCAAAAAA GCGAGAAGATTGTACAGAAATGTGACAGGAAGCATTTCTGTACAATCTT CTCG-3′) and pLCG-shAK2 (sense: 5′-TTTTGGAGCTAATTGAGAAGAATTGC TTCCTGTCACAATTCTTCTCAATTAGCTCCATTTTTTG-3′, antisense: 5′-AATTCAAAAAATGGAGCTAATTGAGAAGAATTGTGACAGGAAGCA ATTCTTCTCAATTAGCTCC-3′).

To obtain lentivirus-encoding green fluorescent protein (as a reporter gene) and shRNA for CD63, 293FT cells (6×10^5) were transfected with pLP1, pLP2, pLP-VSVG and pLCG-shRNA by using Lipofectamine 2000 (Invitrogen, Carlsbad, CA, USA) as per the manufacturer's protocol (Invitrogen). After 24- and 48-h incubations, lentivirus-encoding shRNA was collected.

BM-derived MCs (1×10^6) or MC/9 cells were transduced with shRNA expression lentivirus stock in the presence of 8 μg ml^{-1} Polybrene (Sigma-Aldrich)[55]. After 24 h, the cells were washed and green fluorescent protein-positive cells were sorted by FACSAria and used for subsequent experiments.

Quantitative real-time-PCR. Total RNA was prepared by using TRIzol (Invitrogen) and reverse transcribed by use of Superscript VILO (Invitrogen), as described. Quantitative reverse transcription–PCR was performed with the LightCycler 480 II (Roche, Mannheim, Germany) and the Universal Probe Library (Roche). Primer sequences are listed in Supplementary Table S1.

Statistical analysis. Statistical analysis was performed by using the unpaired two-tailed Student's *t*-test and Welch's *t*-test. The data are presented as means±s.e.m.

References

1. Abraham, C. & Cho, J. H. Inflammatory bowel disease. *N Engl. J. Med.* **361,** 2066–2078 (2009).
2. Strober, W. & Fuss, I. J. Proinflammatory cytokines in the pathogenesis of inflammatory bowel diseases. *Gastroenterology* **140,** 1756–1767 (2011).
3. Alvarez-Errico, D., Lessmann, E. & Rivera, J. Adapters in the organization of mast cell signaling. *Immunol. Rev.* **232,** 195–217 (2009).
4. Bischoff, S. C. Role of mast cells in allergic and non-allergic immune responses: comparison of human and murine data. *Nat. Rev. Immunol.* **7,** 93–104 (2007).
5. Galli, S. J., Borregaard, N. & Wynn, T. A. Phenotypic and functional plasticity of cells of innate immunity: macrophages, mast cells and neutrophils. *Nat. Immunol.* **12,** 1035–1044 (2011).
6. He, S. H. Key role of mast cells and their major secretory products in inflammatory bowel disease. *World J. Gastroenterol.* **10,** 309–318 (2004).
7. Surprenant, A. & North, R. A. Signaling at purinergic P2X receptors. *Annu. Rev. Physiol.* **71,** 333–359 (2009).

8. Erlinge, D. P2Y receptors in health and disease. *Adv. Pharmacol.* **61,** 417–439 (2011).
9. Wilhelm, K. *et al.* Graft-versus-host disease is enhanced by extracellular ATP activating P2X7R. *Nat. Med.* **16,** 1434–1438 (2010).
10. Weber, F. C. *et al.* Lack of the purinergic receptor P2X(7) results in resistance to contact hypersensitivity. *J. Exp. Med.* **207,** 2609–2619 (2010).
11. Muller, T. *et al.* A potential role for P2X7R in allergic airway inflammation in mice and humans. *Am. J. Respir. Cell Mol. Biol.* **44,** 456–464 (2011).
12. Sudo, N. *et al.* Extracellular ATP activates mast cells via a mechanism that is different from the activation induced by the cross-linking of Fc receptors. *J. Immunol.* **156,** 3970–3979 (1996).
13. Furuno, T., Teshima, R., Kitani, S., Sawada, J. & Nakanishi, M. Surface expression of CD63 antigen (AD1 antigen) in P815 mastocytoma cells by transfected IgE receptors. *Biochem. Biophys. Res. Commun.* **219,** 740–744 (1996).
14. Rijnierse, A., Koster, A. S., Nijkamp, F. P. & Kraneveld, A. D. Critical role for mast cells in the pathogenesis of 2,4-dinitrobenzene-induced murine colonic hypersensitivity reaction. *J. Immunol.* **176,** 4375–4384 (2006).
15. Kaser, A., Zeissig, S. & Blumberg, R. S. Inflammatory bowel disease. *Annu. Rev. Immunol.* **28,** 573–621 (2010).
16. Feyerabend, T. B. *et al.* Cre-mediated cell ablation contests mast cell contribution in models of antibody- and T cell-mediated autoimmunity. *Immunity* **35,** 832–844 (2011).
17. Otsuka, A. *et al.* Requirement of interaction between mast cells and skin dendritic cells to establish contact hypersensitivity. *PLoS One* **6,** e25538 (2011).
18. Sawaguchi, M. *et al.* Role of mast cells and basophils in IgE responses and in allergic airway hyperresponsiveness. *J. Immunol.* **188,** 1809–1818 (2012).
19. Fiorucci, S. *et al.* Importance of innate immunity and collagen binding integrin α1β1 in TNBS-induced colitis. *Immunity* **17,** 769–780 (2002).
20. Yoshimoto, T. & Nakanishi, K. Roles of IL-18 in basophils and mast cells. *Allergol. Int.* **55,** 105–113 (2006).
21. Pastorelli, L. *et al.* Epithelial-derived IL-33 and its receptor ST2 are dysregulated in ulcerative colitis and in experimental Th1/Th2 driven enteritis. *Proc. Natl Acad. Sci. USA* **107,** 8017–8022 (2010).
22. Kurashima, Y. *et al.* Sphingosine 1-phosphate-mediated trafficking of pathogenic Th2 and mast cells for the control of food allergy. *J. Immunol.* **179,** 1577–1585 (2007).
23. Nicke, A. *et al.* A functional P2X7 splice variant with an alternative transmembrane domain 1 escapes gene inactivation in P2X7 knock-out mice. *J. Biol. Chem.* **284,** 25813–25822 (2009).
24. Smart, M. L. *et al.* P2X7 receptor cell surface expression and cytolytic pore formation are regulated by a distal C-terminal region. *J. Biol. Chem.* **278,** 8853–8860 (2003).
25. Di Virgilio, F. Liaisons dangereuses: $P2X_7$ and the inflammasome. *Trends Pharmacol. Sci.* **28,** 465–472 (2007).
26. Mizutani, H., Schechter, N., Lazarus, G., Black, R. A. & Kupper, T. S. Rapid and specific conversion of precursor interleukin 1β (IL-1β) to an active IL-1 species by human mast cell chymase. *J. Exp. Med.* **174,** 821–825 (1991).
27. Yegutkin, G. G. Nucleotide- and nucleoside-converting ectoenzymes: important modulators of purinergic signalling cascade. *Biochim. Biophys. Acta.* **1783,** 673–694 (2008).
28. Locovei, S., Bao, L. & Dahl, G. Pannexin 1 in erythrocytes: function without a gap. *Proc. Natl Acad. Sci. USA* **103,** 7655–7659 (2006).
29. Kang, J. *et al.* Connexin 43 hemichannels are permeable to ATP. *J. Neurosci.* **28,** 4702–4711 (2008).
30. Burrell, H. E. *et al.* Human keratinocytes release ATP and utilize three mechanisms for nucleotide interconversion at the cell surface. *J. Biol. Chem.* **280,** 29667–29676 (2005).
31. Foger, N. *et al.* Differential regulation of mast cell degranulation versus cytokine secretion by the actin regulatory proteins Coronin1a and Coronin1b. *J. Exp. Med.* **208,** 1777–1787 (2011).
32. Salamon, P. *et al.* Human mast cells release oncostatin M on contact with activated T cells: possible biologic relevance. *J. Allergy Clin. Immunol.* **121,** 448–455 e5 (2008).
33. Bento, A. F. *et al.* The selective nonpeptide CXCR2 antagonist SB225002 ameliorates acute experimental colitis in mice. *J. Leukoc. Biol.* **84,** 1213–1221 (2008).
34. Luo, M., Jones, S. M., Peters-Golden, M. & Brock, T. G. Nuclear localization of 5-lipoxygenase as a determinant of leukotriene B4 synthetic capacity. *Proc. Natl Acad. Sci. USA* **100,** 12165–12170 (2003).
35. Nigrovic, P. A. *et al.* Genetic inversion in mast cell-deficient *Wsh* mice interrupts corin and manifests as hematopoietic and cardiac aberrancy. *Am. J. Pathol.* **173,** 1693–1701 (2008).
36. Cesaro, A. *et al.* Amplification loop of the inflammatory process is induced by P2X7R activation in intestinal epithelial cells in response to neutrophil transepithelial migration. *Am. J. Physiol. Gastrointest Liver Physiol.* **299,** G32–G42 (2010).
37. Schenk, U. *et al.* ATP inhibits the generation and function of regulatory T cells through the activation of purinergic P2X receptors. *Sci. Signal* **4,** ra12 (2011).
38. Atarashi, K. *et al.* ATP drives lamina propria T_H17 cell differentiation. *Nature* **455,** 808–812 (2008).
39. Wareham, K., Vial, C., Wykes, R. C., Bradding, P. & Seward, E. P. Functional evidence for the expression of P2X1, P2X4 and P2X7 receptors in human lung mast cells. *Br. J. Pharmacol.* **157,** 1215–1224 (2009).
40. Piccini, A. *et al.* ATP is released by monocytes stimulated with pathogen-sensing receptor ligands and induces IL-1β and IL-18 secretion in an autocrine way. *Proc. Natl Acad. Sci. USA* **105,** 8067–8072 (2008).
41. Friedman, D. J. *et al.* From the Cover: CD39 deletion exacerbates experimental murine colitis and human polymorphisms increase susceptibility to inflammatory bowel disease. *Proc. Natl Acad. Sci. USA* **106,** 16788–16793 (2009).
42. Feng, C., Mery, A. G., Beller, E. M., Favot, C. & Boyce, J. A. Adenine nucleotides inhibit cytokine generation by human mast cells through a Gs-coupled receptor. *J. Immunol.* **173,** 7539–7547 (2004).
43. Louis, N. A. *et al.* Control of IFN-αA by CD73: implications for mucosal inflammation. *J. Immunol.* **180,** 4246–4255 (2008).
44. Rijnierse, A., Koster, A. S., Nijkamp, F. P. & Kraneveld, A. D. TNF-α is crucial for the development of mast cell-dependent colitis in mice. *Am. J. Physiol. Gastrointest. Liver Physiol.* **291,** G969–G976 (2006).
45. Cuzzocrea, S. *et al.* 5-Lipoxygenase modulates colitis through the regulation of adhesion molecule expression and neutrophil migration. *Lab. Invest.* **85,** 808–822 (2005).
46. Waddell, A. *et al.* Colonic eosinophilic inflammation in experimental colitis is mediated by $Ly6C^{high}$ $CCR2^{+}$ inflammatory monocyte/macrophage-derived CCL11. *J. Immunol.* **186,** 5993–6003 (2011).
47. Chen, Y. *et al.* Purinergic signaling: a fundamental mechanism in neutrophil activation. *Sci. Signal* **3,** ra45 (2010).
48. Kuida, K. *et al.* Altered cytokine export and apoptosis in mice deficient in interleukin-1β converting enzyme. *Science* **267,** 2000–2003 (1995).
49. Tsai, M., Grimbaldeston, M. A., Yu, M., Tam, S. Y. & Galli, S. J. Using mast cell knock-in mice to analyze the roles of mast cells in allergic responses *in vivo*. *Chem. Immunol. Allergy* **87,** 179–197 (2005).
50. Wirtz, S., Neufert, C., Weigmann, B. & Neurath, M. F. Chemically induced mouse models of intestinal inflammation. *Nat. Protoc.* **2,** 541–546 (2007).
51. Ransford, G. A. *et al.* Pannexin 1 contributes to ATP release in airway epithelia. *Am. J. Respir. Cell Mol. Biol.* **41,** 525–534 (2009).
52. Kunisawa, J. *et al.* Sphingosine 1-phosphate dependence in the regulation of lymphocyte trafficking to the gut epithelium. *J. Exp. Med.* **204,** 2335–2348 (2007).
53. Nochi, T. *et al.* A novel M cell-specific carbohydrate-targeted mucosal vaccine effectively induces antigen-specific immune responses. *J. Exp. Med.* **204,** 2789–2796 (2007).
54. Yu, J. Y., DeRuiter, S. L. & Turner, D. L. RNA interference by expression of short-interfering RNAs and hairpin RNAs in mammalian cells. *Proc. Natl Acad. Sci. USA* **99,** 6047–6052 (2002).
55. Haraguchi, T., Ozaki, Y. & Iba, H. Vectors expressing efficient RNA decoys achieve the long-term suppression of specific microRNA activity in mammalian cells. *Nucleic Acids Res.* **37,** e43 (2009).

Acknowledgements

We thank Drs T. Kitamura and J. Kitaura (The University of Tokyo) for discussions and for providing reagents; Dr H. Suto (Juntendo University) for providing *Kit* $^{W\text{-}sh/W\text{-}sh}$ mice; Dr S. Nakae (The University of Tokyo) for advice on analysing *Kit* $^{W\text{-}sh/W\text{-}sh}$ mice; Drs S. Ohmi, M. Oyama, H. Hata and C. Takamura (The University of Tokyo) for protein analysis; and Dr A. Uozumi, I. Ishikawa and M. Mejima (The University of Tokyo), Drs F. Ishikawa and Y. Saito (RCAI) for technical advice. This work was supported by grants from: the Ministry of Education, Science, Sports and Technology of Japan (Grant-in Aid for Scientific Research S (23229004 to H.K.), for Young Scientists A (22689015 to J.K.), for Scientific Research on Innovative Areas (23116506 to J.K.), for Scientific Research on Priority Areas (19059003 to H.K.), for Challenging Exploratory Research (24659217 to J.K.), Leading-edge Research Infrastructure Program (J.K. and H.K.); the Young Researcher Overseas Visits Program for Vitalizing Brain Circulation of the Japan Society for the Promotion of Science (JSPS; J.K., H.K., Y.K., T.N.), and for JSPS Fellows (021-07124 to Y.K.); the Ministry of Health and Welfare of Japan (J.K. and H.K.); the Global Center of Excellence Program of the Center of Education and Research for Advanced Genome-based Medicine (H.K.); the Program for Promotion of Basic and Applied Research for Innovations in Bio-oriented Industry (BRAIN to J.K.); and the Yakult Bio-Science Foundation (J.K.).

Author contributions

Y.K. conducted the research, performed experiments and wrote the manuscript; T.A. and K.F. performed gene expression and animal experiments; T.N. conducted the mAb experiment; H.T., H. Iba, T.H., M.K. and S.S. contributed to the experimental design and data analysis; S.N. and H. Iijima obtained clinical samples and J.K. and H.K. supervised the project and wrote the manuscript. JK should be contacted for material requests.

Additional information

Supplementary Information accompanies this paper at http://www.nature.com/naturecommunications

Competing financial interests: The authors declare no competing financial interests.

Reprints and permission information is available online at http://npg.nature.com/reprintsandpermissions/

How to cite this article: Kurashima, Y. *et al.* Extracellular ATP mediates mast cell-dependent intestinal inflammation through P2X7 purinoceptors. *Nat. Commun.* 3:1034 doi: 10.1038/ncomms2023 (2012).

frontiers in IMMUNOLOGY

REVIEW ARTICLE
published: 02 April 2012
doi: 10.3389/fimmu.2012.00065

Alcaligenes is commensal bacteria habituating in the gut-associated lymphoid tissue for the regulation of intestinal IgA responses

Jun Kunisawa[1,2]* and Hiroshi Kiyono[1,2,3,4]*

[1] Division of Mucosal Immunology, Department of Microbiology and Immunology, Institute of Medical Science, The University of Tokyo, Tokyo, Japan
[2] Department of Medical Genome Science, Graduate School of Frontier Science, The University of Tokyo, Tokyo, Japan
[3] Graduate School of Medicine, The University of Tokyo, Tokyo, Japan
[4] Core Research for Evolutional Science and Technology, Japan Science and Technology Agency, Tokyo, Japan

Edited by:
Nils Yngve Lycke, University of Gothenburg, Sweden

Reviewed by:
Paul King, Monash University, Australia
Hiroshi Ohno, RIKEN, Japan

***Correspondence:**
Jun Kunisawa and Hiroshi Kiyono, Division of Mucosal Immunology, Department of Microbiology and Immunology, Institute of Medical Science, The University of Tokyo, Tokyo, Japan.
e-mail: kunisawa@ims.u-tokyo.ac.jp; kiyono@ims.u-tokyo.ac.jp

Secretory-immunoglobulin A (S-IgA) plays an important role in immunological defense in the intestine. It has been known for a long time that microbial stimulation is required for the development and maintenance of intestinal IgA production. Recent advances in genomic technology have made it possible to detect uncultivable commensal bacteria in the intestine and identify key bacteria in the regulation of innate and acquired mucosal immune responses. In this review, we focus on the immunological function of Peyer's patches (PPs), a major gut-associated lymphoid tissue, in the induction of intestinal IgA responses and the unique immunological interaction of PPs with commensal bacteria, especially *Alcaligenes*, a unique indigenous bacteria habituating inside PPs.

Keywords: Peyer's patch, IgA, commensal bacteria

INTRODUCTION

Secretory-immunoglobulin A (S-IgA) is predominantly observed in the intestine where it participates in immune defense (Mestecky et al., 2005; Brandtzaeg, 2010). S-IgA inhibits adherence of pathogens to host epithelial cells in the intestinal lumen and neutralizes pathogenic toxins by binding to the toxins' biologically active sites. Based on the immunological importance of S-IgA in immunosurveillance in the intestine, the development of oral vaccines has focused on the induction of antigen-specific S-IgA responses (Kunisawa et al., 2007). In addition to the immunosurveillance in the intestine, S-IgA antibody contributes to the establishment of beneficial gut commensal microbiota and thus dysfunction of S-IgA formation resulted in the alteration of normal bacterial flora (e.g., the reduction of Lactobacillus and increase of segmented filamentous bacteria, SFB; Suzuki et al., 2004).

Peyer's patches (PPs) are major gut-associated lymphoid tissue (GALT) where intestinal IgA responses are initiated and regulated by unique immunological crosstalk via cytokines [e.g., interleukin-4 (IL-4), IL-6, IL-21, and transforming growth factor-β (TGF-β)] and cell–cell interactions (e.g., via CD40/CD40 ligand interactions) among dendritic, T, and B cells (Kunisawa et al., 2008; Fagarasan et al., 2010). Thus, oral delivery of antigens to PPs is considered an important strategy for the effective induction of antigen-specific intestinal IgA responses (Kunisawa et al., 2011).

In addition to host-derived factors, microbial stimulation is also required for the maximum production of S-IgA in the intestine (Cebra et al., 2005). Indeed, germ-free (GF) mice have decreased intestinal IgA responses with immature structure of GALT when compared with mice housed under SPF or conventional conditions (Weinstein and Cebra, 1991). Although it was reported that some commensal bacteria [e.g., SFB and altered Schaedler flora (ASF), a combined eight culturable bacteria] and bacterial products (e.g., peptidoglycan, CpG oligonucleotide, and LPS) stimulated the intestinal IgA production (Michalek et al., 1983; Talham et al., 1999; Butler et al., 2005), it is obscure which bacteria is involved in this process indigenously. Because predominant commensal bacteria in the intestine is uncultivable, it was difficult to determine by culture-based method which bacteria regulated specific immune responses. However, recent advances in the genomic analysis allowed us to identify the uncultivable bacteria, which revealed key bacteria in the regulation of specific immune responses (Ivanov et al., 2009; Atarashi et al., 2011) as well as the development of immune diseases (Chow et al., 2010; Hill and Artis, 2010). Using genomic and immunological methods, we recently found that the microbial community inside PPs is different from those on the epithelium of PPs or in the intestinal lumen (Obata et al., 2010).

In this review, we discuss initially the immunological features of PPs in the induction and regulation of intestinal IgA responses. In the later part, we focus on the unique cross-communication between PPs and habitat commensal bacteria, *Alcaligenes*, a unique indigenous bacteria habituating inside PPs and regulating dendritic cells (DCs) for the efficient production of intestinal IgA.

IMMUNOLOGICAL FEATURES OF PEYER'S PATCHES

In the intestine, GALT comprise several different, organized lymphoid structures (Spencer et al., 2009; Fagarasan et al., 2010). Among them, PPs are the largest and most well-characterized sites

for the initiation of intestinal IgA responses, especially responses to T cell-dependent antigens (Kunisawa et al., 2008; Fagarasan et al., 2010). There are generally 8–10 PPs in the mouse small intestine and hundreds in the human small intestine. Each PP is composed of several B cell-rich follicles surrounded by a mesh-like structure consisting of T cells known as the interfollicular region (**Figure 1**).

Inside PPs, antigen-sampling M cells located in the follicle-associated epithelium transport luminal antigens to DCs situated in the subepithelium region (Neutra et al., 2001), which then form clusters with T-, B-, and stromal cells in the germinal centers and promote μ-to-α-class-switch recombination of B cells with the help of cytokines such as IL-4, IL-21, and TGF-β (Fagarasan et al., 2010). Upon immunoglobulin class-switching from μ to α, IgA-committed B cells (IgA^+ B cells) begin to express type 1 sphingosine-1-phosphate receptor, CCR9, and α4β7 integrin, allowing them to depart from the PPs and subsequently traffic to the intestinal lamina propria (Mora et al., 2006; Gohda et al., 2008). In the intestinal lamina propria, they further differentiate into IgA-secreting plasma cells under the influence of terminal differentiation factors (e.g., IL-6; Cerutti et al., 2011). DCs play a key role in these processes. For instance, nitric oxide, TGF-β, APRIL, and BAFF produced by TNF-α/iNOS-producing DCs (Tip-DCs) promotes IgA production (Tezuka et al., 2007). Also, DCs in the PPs metabolite vitamin A and produce retinoic acid, which induces the expression of gut-homing receptors (CCR9, and α4β7 integrin) on activated B and T cells (Iwata et al., 2004; Mora et al., 2006). Retinoic acid also induces the preferential differentiation into regulatory T (Treg) cells (Hall et al., 2011), and some of Treg cells differentiated into follicular helper T cells to promote IgA production in the PPs (Tsuji et al., 2009).

The identification of the molecular pathway of PP organogenesis allowed the establishment of PP-deficient mice through the loss of any part of this pathway (Nishikawa et al., 2003). Notably, disruption of the PP organogenesis pathway by blockade of tissue genesis cytokine receptor signaling [IL-7R and/or lymphotoxin-β receptor (LTβR)] during a limited fetus time period results in the selective loss of PPs without affecting other lymphoid tissue organogenesis (Yoshida et al., 1999). Experiments with PP-deficient mice showed that the dependency on PPs in the induction of antigen-specific IgA responses depends on the form of the antigen. For instance, the PP-deficient mice failed to develop antigen-specific IgA responses against orally administered antigens in particle form, but retained their ability to respond to soluble forms of antigens (Yamamoto et al., 2000; Kunisawa et al., 2002). It was also reported that lamina propria DCs are capable of initiating systemic IgG responses, whereas antigen transport by M cells into the PPs is required for the induction of intestinal IgA production (Martinoli et al., 2007). This is consistent with another finding that DCs in the PPs are responsible for intestinal IgA production (Fleeton et al., 2004). Therefore, PPs are considered to be one of the major sites for the initiation of intestinal antigen-specific IgA responses.

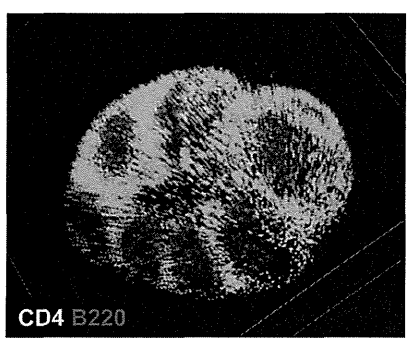

FIGURE 1 | Microarchitecture of murine Peyer's patches. Purified T cells (green) and B cells (red) were chemically labeled with carboxyfluorescein succinimidyl ester and carboxy-SNARF-1, respectively, and adoptively transferred into mice. Fifteen hours after the transfer, cell distribution in the Peyer's patches was observed at the whole-tissue level by using macro-confocal microscopy.

EFFECT OF MICROBIAL STIMULATION ON THE PRODUCTION OF INTESTINAL IgA

It is well known that microbial stimulation is required for the full production of S-IgA in the intestine. Indeed, GF mice have decreased intestinal IgA responses when compared with mice housed under SPF or conventional conditions (Cebra et al., 2005). Studies using mono-associated GF mice with SFB have demonstrated that only a minor proportion of the total intestinal IgA is reactive to mono-associated bacteria (Talham et al., 1999). In addition, bacterial products produced by commonly expressed on commensal bacteria (e.g., peptidoglycan, CpG oligonucleotide, and LPS) stimulated the intestinal IgA production (Michalek et al., 1983; Butler et al., 2005). In contrast, a recent study using reversible colonization of GF mice with genetically engineered *E. coli* showed that intestinal IgA induced in those mice bound to parent strain but not other bacteria (Hapfelmeier et al., 2010). Therefore, it remains unclear whether intestinal IgA responses induced by commensal bacteria is mediated by polyclonal stimulation and/or by B cell receptors specific for microbial antigens.

As one mechanism of impaired IgA production of GF mice, it was reported that GF mice have structurally immature GALT (e.g., PPs and ILFs) when compared with SPF mice (Weinstein and Cebra, 1991; Hamada et al., 2002). In the PPs, several key pathways for the IgA production require microbial stimulation. For example, Tip-DCs enhance the IgA production by producing nitric oxide, TGF-β, APRIL, and BAFF, which requires microbial stimulation through innate receptors (Tezuka et al., 2007). Indeed, the number of Tip-DCs was much reduced in the intestine of GF and MyD88-deficient mice (Tezuka et al., 2007). Another cell involved the microbe-dependent IgA production is non-hematopoietic follicular DCs (FDCs). It was reported that microbial stimulation of FDCs resulted in expressing chemokine CXCL13, BAFF, and TGF-β for the germinal center formation and B cell class-switching from IgM to IgA (Suzuki et al., 2010).

ALCALIGENES IS A UNIQUE INDIGENOUS BACTERIA INSIDE PPs

Recent advances in genomic technology make it possible to detect commensal bacteria in the intestine, allowing identification of key bacteria involved in the regulation of specific immune responses. For example, SFB was identified as commensal bacteria inducing

Th17 cells (Ivanov et al., 2009), whereas colonic regulatory T cells were induced by *Clostridium* clusters IV and XIV (Atarashi et al., 2011). These commensal bacteria localize at the surface of intestinal epithelium, but we supposed that the immunological crosstalk between host and commensal bacteria might establish in the regulation of intestinal IgA responses in the GALT. In this issue, we analyzed the composition of the microbial community inside PPs and identified *Alcaligenes* as a major commensal bacteria uniquely locating inside PPs (Obata et al., 2010).

By using the 16S rRNA clone library method, SFB are the predominant commensal bacteria co-habitat on FAE of PPs as like small intestinal epithelium. Although the FAE consisted with antigen-sampling M cells, SFB was not found inside of PPs. Instead, *Alcaligenes* are predominant bacteria inside PPs. The result obtained by the 16S rRNA analysis was further confirmed by fluorescence *in situ* hybridization (FISH) method and thus *Alcaligenes* are present exclusively inside PPs, not on the FAE of PPs, and intestinal villous epithelium and intestinal lamina propria (**Figure 2**). Of note, the preferential presence of *Alcaligenes* was observed not only in mouse but also in monkey and human (Obata et al., 2010). One of interesting but unresolved questions is the species specificity of *Alcaligenes*. We are now investigating whether *Alcaligenes* isolated from human or monkey colonize in the PPs to promote IgA production when they are orally fed to GF mice. Inside PPs, a proportion of the *Alcaligenes* seemed to be alive in mice. The presence and growth of *Alcaligenes* were detected in the PPs of GF mice after adoptive transfer of PP homogenates containing *Alcaligenes* from SPF mice. These findings suggest that *Alcaligenes* are indigenous bacteria ubiquitously living inside the PPs of various mammalian species.

ANTIBODY-MEDIATED RECIPROCAL INTERACTION BETWEEN *ALCALIGENES* AND THE HOST IMMUNE SYSTEM

As mentioned above, M cells located on the FAE of PPs transport luminal bacteria into DCs locating at the subepithelial region of FAE (Neutra et al., 2001). 16S rRNA clone library methods consistently revealed that DCs in the PPs predominantly contain *Alcaligenes*, whereas these bacteria are rarely detected in DCs isolated from other lymphoid tissues (e.g., spleen and mesenteric lymph nodes; Obata et al., 2010). We examined the immunological effects of *Alcaligenes* on DCs and found that the production of IgA-enhancing cytokines such as IL-6, TGF-β, and BAFF was increased when DCs isolated from the PPs of GF mice were stimulated with *Alcaligenes* (Obata et al., 2010). Several lines of evidence have revealed that immunological functions of DCs are different between intestinal and other lymphoid tissues (reviewed in Rescigno, 2010), we are now investigating whether immune stimulatory functions of *Alcaligenes* is specific for the PP DCs or not.

In agreement with the uptake of *Alcaligenes* and subsequent production of IgA-enhancing cytokines by DCs, *Alcaligenes*-specific IgA-forming cells were frequently observed in PPs, and consequent IgA production was noted in the intestinal lumen of SPF mice, but not GF mice (Obata et al., 2010). Although biological role of *Alcaligenes*-specific IgA antibody remains to be elucidated, the antibody might be involved in the creation of intratissue co-habitation of *Alcaligenes* in PPs. To this end, the number of *Alcaligenes* inside PPs is decreased in B cell-deficient CBA/N xid and IgA-deficient mice compared with wild-type mice (Obata et al., 2010). Therefore, it is interesting to suggest that *Alcaligenes*-specific IgA antibody mediates the uptake and presence of *Alcaligenes* in the PPs. Since M cells express IgA receptors

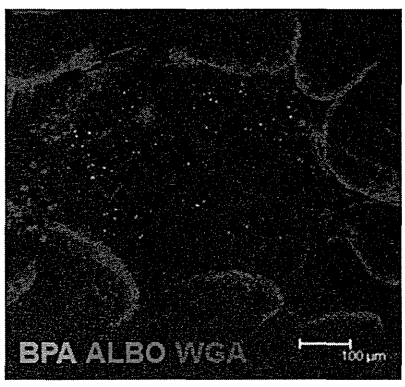

FIGURE 2 | Microarchitecture of murine Peyer's patches. Whole-mount fluorescence *in situ* hybridization was performed to visually analyze the presence of *Alcaligenes* inside PPs. Both BPA and ALBO34a were used as specific probes for *Alcaligenes*. Wheat germ agglutinin (WGA), an *N*-acetylglucosamine-specific lectin, was used to detect epithelial cells. Scale bar indicates 100 μm.

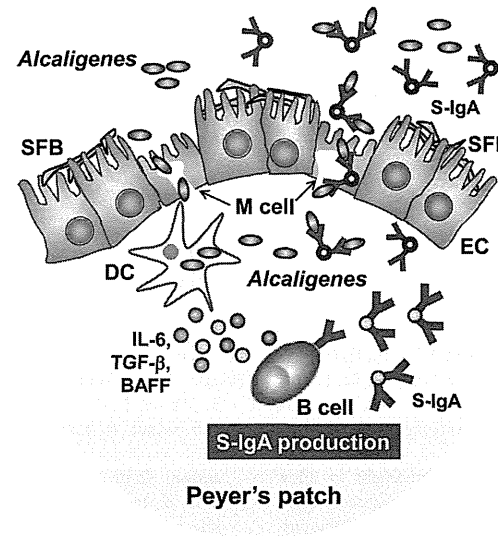

FIGURE 3 | *Alcaligenes* mediates symbiotic communication inside Peyer's patches. On the follicle-associated epithelium of PPs, segmented filamentous bacteria (SFB) is predominantly observed. In contrast, *Alcaligenes* specifically localizes inside Peyer's patches, where some are taken up by dendritic cells (DCs). Stimulation by *Alcaligenes* prompts the DCs to produce IgA-enhancing cytokines [e.g., interleukin-6 (IL-6), transforming growth factor-β (TGF-β)], and B cell activating factor (BAFF), which enhance the intestinal IgA response. The intestinal IgA includes *Alcaligenes*-specific IgA, which might mediate the preferential uptake and presence of *Alcaligenes* in the PPs. The uptake is presumably mediated by M cells.

(Mantis et al., 2002), one possibility is that *Alcaligenes* coated with the *Alcaligenes*-specific antibody are taken up into PPs through M cells. Further, the antigen-specific IgA coating on *Alcaligenes* might be beneficial for the bacteria to create the co-habitation niche since IgA antibody has been shown to non-inflammatory antibody (Mestecky et al., 2005).

CONCLUSION

In this review, we discussed a new concept of symbiotic communication in PPs that is mediated by commensal bacteria-specific IgA antibody. *Alcaligenes*-specific antibodies may mediate the uptake and the presence of *Alcaligenes* in the PPs, and the co-habitation of *Alcaligenes* within the PPs is one of the key factors to promote the intestinal IgA production by enhancing the production of IgA-enhancing cytokines from DCs (**Figure 3**). We still have various questions regarding this co-habitation of *Alcaligenes* in the PPs. For example, it remains unclear whether the presence of *Alcaligenes* inside of PPs is physiologically beneficial or harmful for the host immune system. In this issue, we are now addressing the microbial community in the PPs of mice and human patients suffering from intestinal immune diseases (e.g., intestinal inflammation and allergy). The biological roles of intra-tissue habitation of *Alcaligenes* in the PPs in the appropriate regulation of mucosal immune responses need to be elucidated. The current goal is to elucidate the mechanisms behind the co-habitation of *Alcaligenes* within PPs, and the exact contribution of *Alcaligenes* to educate and guide mucosal immunocompetent cells especially DCs in the PPs for the development, maturation and maintenance of the appropriate host immune system. These studies will provide novel molecular and cellular mechanisms of symbiotic communication with commensal bacteria in the regulation of host immunity.

ACKNOWLEDGMENTS

We thank Dr. T. Obata for his contribution to all works related to *Alcaligenes*, Drs. Y. Benno and M. Sakamoto (RIKEN BioResource Center), and Drs. Y. Umesaki, T. Matsuki, H. Setoyama (Yakult Central Institute for Microbiological Research) for their constructive discussions, technical advice, and supports on microbial analyses, and Dr. H. Iijima (Osaka University) for providing human samples. The work related to this review was supported by grants from the Ministry of Education, Culture, Sports, Science and Technology of Japan [Grant-in-Aid for Young Scientists A (22689015 to Jun Kunisawa), for Scientific Research on Innovative Areas (23116506 to Jun Kunisawa), for Scientific Research S (23229004 to Hiroshi Kiyono), and for Scientific Research on Priority Area (19059003 to Hiroshi Kiyono)]; the Ministry of Health and Welfare of Japan (to Jun Kunisawa and Hiroshi Kiyono); the Global Center of Excellence Program of the Center of Education and Research for Advanced Genome-based Medicine (to Hiroshi Kiyono); the Program for Promotion of Basic and Applied Researches for Innovations in Bio-oriented Industry (to Jun Kunisawa); and the Yakult Bio-Science Foundation (to Jun Kunisawa).

REFERENCES

Atarashi, K., Tanoue, T., Shima, T., Imaoka, A., Kuwahara, T., Momose, Y., Cheng, G., Yamasaki, S., Saito, T., Ohba, Y., Taniguchi, T., Takeda, K., Hori, S., Ivanov, I. I., Umesaki, Y., Itoh, K., and Honda, K. (2011). Induction of colonic regulatory T cells by indigenous *Clostridium* species. *Science* 331, 337–341.

Brandtzaeg, P. (2010). Function of mucosa-associated lymphoid tissue in antibody formation. *Immunol. Invest.* 39, 303–355.

Butler, J. E., Francis, D. H., Freeling, J., Weber, P., and Krieg, A. M. (2005). Antibody repertoire development in fetal and neonatal piglets. IX. Three pathogen-associated molecular patterns act synergistically to allow germfree piglets to respond to type 2 thymus-independent and thymus-dependent antigens. *J. Immunol.* 175, 6772–6785.

Cebra, J. J., Jiang, H. Q., Boiko, N. V., and Tlaskalva-Hogenova, H. (2005). "The role of mucosal microbiota in the development, maintenance, and pathologies of the mucosal immune system," in *Mucosal Immunology*, 3rd Edn, eds J. Mestecky, M. E. Lamm, W. Strober, J. Bienenstock, J. R. Mcghee, and L. Mayer (San Diego: Academic Press), 335–368.

Cerutti, A., Chen, K., and Chorny, A. (2011). Immunoglobulin responses at the mucosal interface. *Annu. Rev. Immunol.* 29, 273–293.

Chow, J., Lee, S. M., Shen, Y., Khosravi, A., and Mazmanian, S. K. (2010). Host-bacterial symbiosis in health and disease. *Adv. Immunol.* 107, 243–274.

Fagarasan, S., Kawamoto, S., Kanagawa, O., and Suzuki, K. (2010). Adaptive immune regulation in the gut: T cell-dependent and T cell-independent IgA synthesis. *Annu. Rev. Immunol.* 28, 243–273.

Fleeton, M. N., Contractor, N., Leon, F., Wetzel, J. D., Dermody, T. S., and Kelsall, B. L. (2004). Peyer's patch dendritic cells process viral antigen from apoptotic epithelial cells in the intestine of reovirus-infected mice. *J. Exp. Med.* 200, 235–245.

Gohda, M., Kunisawa, J., Miura, F., Kagiyama, Y., Kurashima, Y., Higuchi, M., Ishikawa, I., Ogahara, I., and Kiyono, H. (2008). Sphingosine 1-phosphate regulates the egress of IgA plasmablasts from Peyer's patches for intestinal IgA responses. *J. Immunol.* 180, 5335–5343.

Hall, J. A., Grainger, J. R., Spencer, S. P., and Belkaid, Y. (2011). The role of retinoic acid in tolerance and immunity. *Immunity* 35, 13–22.

Hamada, H., Hiroi, T., Nishiyama, Y., Takahashi, H., Masunaga, Y., Hachimura, S., Kaminogawa, S., Takahashi-Iwanaga, H., Iwanaga, T., Kiyono, H., Yamamoto, H., and Ishikawa, H. (2002). Identification of multiple isolated lymphoid follicles on the antimesenteric wall of the mouse small intestine. *J. Immunol.* 168, 57–64.

Hapfelmeier, S., Lawson, M. A., Slack, E., Kirundi, J. K., Stoel, M., Heikenwalder, M., Cahenzli, J., Velykoredko, Y., Balmer, M. L., Endt, K., Geuking, M. B., Curtiss, R. III, Mccoy, K. D., and Macpherson, A. J. (2010). Reversible microbial colonization of germ-free mice reveals the dynamics of IgA immune responses. *Science* 328, 1705–1709.

Hill, D. A., and Artis, D. (2010). Intestinal bacteria and the regulation of immune cell homeostasis. *Annu. Rev. Immunol.* 28, 623–667.

Ivanov, I. I., Atarashi, K., Manel, N., Brodie, E. L., Shima, T., Karaoz, U., Wei, D., Goldfarb, K. C., Santee, C. A., Lynch, S. V., Tanoue, T., Imaoka, A., Itoh, K., Takeda, K., Umesaki, Y., Honda, K., and Littman, D. R. (2009). Induction of intestinal Th17 cells by segmented filamentous bacteria. *Cell* 139, 485–498.

Iwata, M., Hirakiyama, A., Eshima, Y., Kagechika, H., Kato, C., and Song, S. Y. (2004). Retinoic acid imprints gut-homing specificity on T cells. *Immunity* 21, 527–538.

Kunisawa, J., Kurashima, Y., and Kiyono, H. (2011). Gut-associated lymphoid tissues for the development of oral vaccines. *Adv. Drug Deliv. Rev.* [Epub ahead of print].

Kunisawa, J., Mcghee, J., and Kiyono, H. (2007). "Mucosal S-IgA enhancement: development of safe and effective mucosal adjuvants and mucosal antigen delivery vehicles," in *Mucosal Immune Defense: Immunoglobulin A*, ed. C. Kaetzel (New York: Kluwer Academic/Plenum Publishers), 346–389.

Kunisawa, J., Nochi, T., and Kiyono, H. (2008). Immunological commonalities and distinctions between airway and digestive immunity. *Trends Immunol.* 29, 505–513.

Kunisawa, J., Takahashi, I., Okudaira, A., Hiroi, T., Katayama, K., Ariyama, T., Tsutsumi, Y., Nakagawa, S., Kiyono, H., and Mayumi, T. (2002). Lack of antigen-specific immune responses in anti-IL-7 receptor α chain antibody-treated Peyer's patch-null mice following intestinal immunization with microencapsulated antigen. *Eur. J. Immunol.* 32, 2347–2355.

Mantis, N. J., Cheung, M. C., Chintalacharuvu, K. R., Rey, J., Corthesy, B., and Neutra, M. R. (2002). Selective adherence of IgA to murine Peyer's patch M cells: evidence for a novel IgA receptor. *J. Immunol.* 169, 1844–1851.

Martinoli, C., Chiavelli, A., and Rescigno, M. (2007). Entry route of *Salmonella typhimurium* directs the type of induced immune response. *Immunity* 27, 975–984.

Mestecky, J., Moro, I., Kerr, M. A., and Woof, J. M. (2005). "Mucosal immunoglobulins," in *Mucosal Immunology*, 3rd Edn, eds J. Mestecky, M. E. Lamm, W. Strober, J. Bienenstock, J. R. Mcghee, and L. Mayer (San Diego: Academic Press), 153–182.

Michalek, S. M., Morisaki, I., Gregory, R. L., Kiyono, H., Hamada, S., and Mcghee, J. R. (1983). Oral adjuvants enhance IgA responses to *Streptococcus mutans*. *Mol. Immunol.* 20, 1009–1018.

Mora, J. R., Iwata, M., Eksteen, B., Song, S. Y., Junt, T., Senman, B., Otipoby, K. L., Yokota, A., Takeuchi, H., Ricciardi-Castagnoli, P., Rajewsky, K., Adams, D. H., and Von Andrian, U. H. (2006). Generation of gut-homing IgA-secreting B cells by intestinal dendritic cells. *Science* 314, 1157–1160.

Neutra, M. R., Mantis, N. J., and Kraehenbuhl, J. P. (2001). Collaboration of epithelial cells with organized mucosal lymphoid tissues. *Nat. Immunol.* 2, 1004–1009.

Nishikawa, S., Honda, K., Vieira, P., and Yoshida, H. (2003). Organogenesis of peripheral lymphoid organs. *Immunol. Rev.* 195, 72–80.

Obata, T., Goto, Y., Kunisawa, J., Sato, S., Sakamoto, M., Setoyama, H., Matsuki, T., Nonaka, K., Shibata, N., Gohda, M., Kagiyama, Y., Nochi, T., Yuki, Y., Fukuyama, Y., Mukai, A., Shinzaki, S., Fujihashi, K., Sasakawa, C., Iijima, H., Goto, M., Umesaki, Y., Benno, Y., and Kiyono, H. (2010). Indigenous opportunistic bacteria inhabit mammalian gut-associated lymphoid tissues and share a mucosal antibody-mediated symbiosis. *Proc. Natl. Acad. Sci. U.S.A.* 107, 7419–7424.

Rescigno, M. (2010). Intestinal dendritic cells. *Adv. Immunol.* 107, 109–138.

Spencer, J., Barone, F., and Dunn-Walters, D. (2009). Generation of immunoglobulin diversity in human gut-associated lymphoid tissue. *Semin. Immunol.* 21, 139–146.

Suzuki, K., Maruya, M., Kawamoto, S., Sitnik, K., Kitamura, H., Agace, W. W., and Fagarasan, S. (2010). The sensing of environmental stimuli by follicular dendritic cells promotes immunoglobulin A generation in the gut. *Immunity* 33, 71–83.

Suzuki, K., Meek, B., Doi, Y., Muramatsu, M., Chiba, T., Honjo, T., and Fagarasan, S. (2004). Aberrant expansion of segmented filamentous bacteria in IgA-deficient gut. *Proc. Natl. Acad. Sci. U.S.A.* 101, 1981–1986.

Talham, G. L., Jiang, H. Q., Bos, N. A., and Cebra, J. J. (1999). Segmented filamentous bacteria are potent stimuli of a physiologically normal state of the murine gut mucosal immune system. *Infect. Immun.* 67, 1992–2000.

Tezuka, H., Abe, Y., Iwata, M., Takeuchi, H., Ishikawa, H., Matsushita, M., Shiohara, T., Akira, S., and Ohteki, T. (2007). Regulation of IgA production by naturally occurring TNF/iNOS-producing dendritic cells. *Nature* 448, 929–933.

Tsuji, M., Komatsu, N., Kawamoto, S., Suzuki, K., Kanagawa, O., Honjo, T., Hori, S., and Fagarasan, S. (2009). Preferential generation of follicular B helper T cells from Foxp3+ T cells in gut Peyer's patches. *Science* 323, 1488–1492.

Weinstein, P. D., and Cebra, J. J. (1991). The preference for switching to IgA expression by Peyer's patch germinal center B cells is likely due to the intrinsic influence of their microenvironment. *J. Immunol.* 147, 4126–4135.

Yamamoto, M., Rennert, P., Mcghee, J. R., Kweon, M. N., Yamamoto, S., Dohi, T., Otake, S., Bluethmann, H., Fujihashi, K., and Kiyono, H. (2000). Alternate mucosal immune system: organized Peyer's patches are not required for IgA responses in the gastrointestinal tract. *J. Immunol.* 164, 5184–5191.

Yoshida, H., Honda, K., Shinkura, R., Adachi, S., Nishikawa, S., Maki, K., Ikuta, K., and Nishikawa, S. I. (1999). IL-7 receptor α^+ CD3- cells in the embryonic intestine induces the organizing center of Peyer's patches. *Int. Immunol.* 11, 643–655.

Conflict of Interest Statement: The authors declare that the research was conducted in the absence of any commercial or financial relationships that could be construed as a potential conflict of interest.

Received: 27 January 2012; paper pending published: 15 February 2012; accepted: 15 March 2012; published online: 02 April 2012.

Citation: Kunisawa J and Kiyono H (2012) Alcaligenes is commensal bacteria habituating in the gut-associated lymphoid tissue for the regulation of intestinal IgA responses. Front. Immun. 3:65. doi: 10.3389/fimmu.2012.00065

This article was submitted to Frontiers in Mucosal Immunity, a specialty of Frontiers in Immunology.

THE JOURNAL OF IMMUNOLOGY

Development of Mature and Functional Human Myeloid Subsets in Hematopoietic Stem Cell-Engrafted NOD/SCID/IL2rγKO Mice

Satoshi Tanaka, Yoriko Saito, Jun Kunisawa, Yosuke Kurashima, Taichi Wake, Nahoko Suzuki, Leonard D. Shultz, Hiroshi Kiyono and Fumihiko Ishikawa

J Immunol published online 18 May 2012
http://www.jimmunol.org/content/early/2012/05/18/jimmunol.1103660

The Journal of Immunology is published twice each month by The American Association of Immunologists, Inc., 9650 Rockville Pike, Bethesda, MD 20814-3994.

Print ISSN: 0022-1767 Online ISSN: 1550-6606.

Published May 18, 2012, doi:10.4049/jimmunol.1103660

Development of Mature and Functional Human Myeloid Subsets in Hematopoietic Stem Cell-Engrafted NOD/SCID/IL2rγKO Mice

Satoshi Tanaka,*,†,‡,§ Yoriko Saito,‡ Jun Kunisawa,*,† Yosuke Kurashima,† Taichi Wake,† Nahoko Suzuki,‡ Leonard D. Shultz,¶ Hiroshi Kiyono,*,†,‖ and Fumihiko Ishikawa‡

Although physiological development of human lymphoid subsets has become well documented in humanized mice, in vivo development of human myeloid subsets in a xenotransplantation setting has remained unevaluated. Therefore, we investigated in vivo differentiation and function of human myeloid subsets in NOD/SCID/IL2rγ^{null} (NSG) mouse recipients transplanted with purified lineage$^-$CD34$^+$CD38$^-$ cord blood hematopoietic stem cells. At 4–6 mo posttransplantation, we identified the development of human neutrophils, basophils, mast cells, monocytes, and conventional and plasmacytoid dendritic cells in the recipient hematopoietic organs. The tissue distribution and morphology of these human myeloid cells were similar to those identified in humans. After cytokine stimulation in vitro, phosphorylation of STAT molecules was observed in neutrophils and monocytes. In vivo administration of human G-CSF resulted in the recruitment of human myeloid cells into the recipient circulation. Flow cytometry and confocal imaging demonstrated that human bone marrow monocytes and alveolar macrophages in the recipients displayed intact phagocytic function. Human bone marrow-derived monocytes/macrophages were further confirmed to exhibit phagocytosis and killing of *Salmonella typhimurium* upon IFN-γ stimulation. These findings demonstrate the development of mature and functionally intact human myeloid subsets in vivo in the NSG recipients. In vivo human myelopoiesis established in the NSG humanized mouse system may facilitate the investigation of human myeloid cell biology including in vivo analyses of infectious diseases and therapeutic interventions. ***The Journal of Immunology*****, 2012, 188: 000–000.**

The use of genetically modified mice has led to significant advances in biomedical research by providing insights into the role of individual genes both in normal physiology and in disease pathogenesis. However, translation of these findings into effective therapies for human diseases has been limited by the gap that exists between murine and human biology. The availability of human samples (e.g., cells and tissues), although supporting successful translation from bench research to clinical medicine, is limited by both logistic and ethical concerns.

Therefore, mice repopulated with human hematopoietic cells through xenogeneic transplantation were developed directly to investigate the human immuno-hematopoietic system in vivo. Based on pioneering work using the Hu-PBL-SCID (1) and SCID-hu (2) systems, investigators have aimed to improve xenotransplantation models using immunodeficient strains of mice as recipients of human hematopoietic stem cells (HSCs) to achieve long-term engraftment of multiple human hematopoietic and immune subsets (3). NOD/SCID mice, established by back-crossing the *scid* mutation onto the NOD strain background, are characterized by partially impaired innate immunity and deficient complement-dependent cytotoxicity and are the gold standard for stable human hematopoietic stem/progenitor cell engraftment (3, 4). The ability of NOD-*scid* mice to support human HSC engraftment is associated with a human-like polymorphism in the IgV domain of the signal regulatory protein-α (*Sirpa*) allele in the NOD strain background resulting in the expression of SIRPα with enhanced binding of human CD47 (5). The interaction between SIRPα and CD47 has previously been implicated in the negative regulation of phagocytosis by macrophages through a "do-not-eat-me signal" (6).

The introduction of IL2r common γ-chain mutations onto the NOD/SCID and BALBc/Rag2KO backgrounds led to the generation of the NOD/SCID/γ_c^{null} (NOG) (7, 8) strain with a truncated IL-2Rγ, the NOD/SCID/IL2rγ^{null} (NSG) (9, 10) strain with a complete IL-2Rγ-null mutation, and BALB/c-Rag2KO/γ_c^{null} mice (11), resulting in more profound defects in innate immunity. In vivo human hematopoietic repopulation through transplantation

*Department of Medical Genome Sciences, Graduate School of Frontier Sciences, The University of Tokyo, Chiba, Japan; †Division of Mucosal Immunology, The Institute of Medical Science, The University of Tokyo, Tokyo, Japan; ‡Research Unit for Human Disease Models, RIKEN Research Center for Allergy and Immunology, Yokohama, Japan; §Nippon Becton Dickinson Company, Tokyo, Japan; ¶The Jackson Laboratory, Bar Harbor, ME; and ‖Core Research for Evolutional Science and Technology, Japan Science and Technology Agency, Tokyo, Japan

Received for publication December 30, 2011. Accepted for publication April 19, 2012.

This work was supported by grants from the Ministry of Education, Culture, Sports, Science and Technology of Japan and from the Takeda Science Foundation (to F.I.); grants from the Ministry of Education, Culture, Sports, Science and Technology of Japan (to H.K. and J.K.); the Program for Promotion of Basic and Applied Researches for Innovations in Bio-oriented Industry (to J.K.); and grants from the National Institutes of Health, the U.S. Army Medical Research Institute of Infectious Diseases, and the Helmsley Foundation (to L.D.S.). Y.K. is a Japan Society for the Promotion of Science fellow.

Address correspondence and reprint requests to Fumihiko Ishikawa, Research Unit for Human Disease Models, RIKEN Research Center for Allergy and Immunology, 1-7-22 Suehiro-cho Tsurumi-ku, Yokohama 230-0045, Japan. E-mail address: f_ishika@rcai.riken.jp

The online version of this article contains supplemental material.

Abbreviations used in this article: BM, bone marrow; CB, cord blood; cDC, conventional dendritic cell; DC, dendritic cell; HSC, hematopoietic stem cell; MNC, mononuclear cell; MOI, multiplicity of infection; PB, peripheral blood; pDC, plasmacytoid dendritic cell; rhG-CSF, recombinant human G-CSF; rhGM-CSF, recombinant human GM-CSF; rhIFN-γ, recombinant human IFN-γ; rhM-CSF, recombinant human M-CSF.

www.jimmunol.org/cgi/doi/10.4049/jimmunol.1103660

of human $CD34^+$ or $CD34^+CD38^-$ HSCs in these severely immunocompromised recipients accelerated human stem cell and immunology research by allowing higher levels of human HSC engraftment, differentiation of human T cells in the murine thymus and secondary lymphoid organs, enhanced maturation of human B cells, and human immune function in vivo (7–12).

Despite these advances, one of the remaining issues to be clarified in humanized mouse research has been the development of human myeloid lineage cells in the host mouse tissues. To date, we and others reported the development of human $CD33^+$ myeloid cells and myeloid subsets in NOG mice, BALB/c-Rag2KO/γ_c^{null} mice, and NSG mice (7, 9, 11, 13). In this study, by using NSG newborns as recipients, we present in vivo differentiation of human myeloid subsets in the bone marrow (BM), spleen, and respiratory tract of NSG mice engrafted with purified $lineage^-CD34^+CD38^-$ human cord blood (CB) HSCs. Human granulocytes (neutrophils, basophils, and mast cells) and APCs (monocytes/macrophages, conventional dendritic cells [cDCs] and plasmacytoid dendritic cells [pDCs]) developing in NSG mice exhibited characteristics of human myeloid cells including morphological features and expression of surface molecules known to be associated with the myeloid cell subsets. Moreover, human myeloid cells developing in the NSG recipients displayed functionality such as responsiveness to cytokine or TLR adjuvant and phagocytic function. The in vivo system supporting the development of mature human myeloid cells with intact function will facilitate the evaluation of human myeloid development from hematopoietic stem/progenitor cells, advance in vivo investigation of human myeloid cell-mediated immune responses against pathogens and malignancies, and will support studies of therapeutic agents.

Materials and Methods

Mice

NOD.Cg-*Prkdc*^{scid}*IL2rg*^{tmlWjl}/Sz (NSG) mice were developed at The Jackson Laboratory by back-crossing a complete null mutation at the *Il2rg* locus onto the NOD.Cg-*Prkdc*^{scid} (NOD/SCID) strain (9, 10). Mice were bred and maintained under defined flora with irradiated food at the animal facility of RIKEN and at The Jackson Laboratory according to guidelines established by the institutional animal committees at each respective institution.

Purification of human HSCs and xenogeneic transplantation

All experiments were performed with authorization from the Institutional Review Board for Human Research at RIKEN Research Center for Allergy and Immunology. CB samples were first separated for mononuclear cells (MNCs) by LSM lymphocyte separation medium (MP Biomedicals). CB MNCs were then enriched for human $CD34^+$ cells by using anti-human CD34 microbeads (Miltenyi Biotec) and sorted for $7AAD^-$lineage(hCD3/hCD4/hCD8/hCD19/hCD56)$^-CD34^+CD38^-$ HSCs using FACSAria (BD Biosciences). To achieve high purity of donor HSCs, doublets were excluded by analysis of forward scatter-height/forward scatter-width and side scatter-height/side scatter-width. The purity of HSCs was higher than 98% after sorting. Newborn (within 2 d of birth) recipients received 150 cGy total body irradiation using a ^{137}Cs-source irradiator, followed by i.v. injection of 1×10^4–3×10^4 sorted HSCs via the facial vein (14). The recipient peripheral blood (PB) harvested from the retro-orbital plexus was evaluated for human hematopoietic engraftment every 3 to 4 wk starting at 6 wk posttransplantation. At 4–6 mo posttransplantation, recipient mice were euthanized for analysis.

Flow cytometry

Erythrocytes in the PB were lysed with Pharm Lyse (BD Biosciences). Single-cell suspensions were prepared from BM and spleen using standard procedures. To isolate MNCs from the lung, lung tissues were carefully excised, teased apart, and dissociated using collagenase (Wako) (15). The following mAbs were used for identifying engraftment of human hematopoietic cells in NSG recipients: anti-human CD3 V450 (clone UCHT1) and PE–Cy5 (HIT3a), anti-hCD4 PE–Cy5 (RPA-T4), anti-hCD8 PE–Cy5 (RPA-T8), anti-hCD11b/Mac-1 Pacific blue (ICRF44), anti-hCD11c allophycocyanin (B-ly6), anti-hCD14 Alexa700 (M5E2), allophycocyanin–H7 and V450 (MϕP9), anti-hCD15 allophycocyanin (HI98) and V450 (MMA), anti-hCD19 PerCP–Cy5.5, PE–Cy5 and PE–Cy7 (SJ25C1), anti-hCD33 PE and PE–Cy7 (p67.6), anti-hCD34 PE–Cy7 (8G12), anti-hCD38 FITC and allophycocyanin (HB7), anti-hCD45, V450 and V500 (HI30), anti-hCD45 AmCyan and allophycocyanin–Cy7 (2D1), anti-hCD56 FITC (NCAM16.2) and PE–Cy5 (B159), anti-hCD114/G-CSFR PE (LMM741), anti-hCD116/GM-CSFR FITC (hGMCSFR-M1), anti-hCD117/c-Kit PerCP–Cy5.5 (104D2), anti-hCD119/IFN-γR PE (GIR-208), anti-hCD123/IL-3R PE and PerCP–Cy5.5 (7G3), anti-hCD284/TLR2 Alexa647 (11G7), anti–HLA-DR allophycocyanin–H7 (L243), anti-mouse CD45 PerCP–Cy5.5 and allophycocyanin–Cy7 (30-F11), all from BD Biosciences; anti-human CD1c/BDCA-1 FITC (AD5-8E7), anti-hCD141/BDCA-3 FITC, PE and allophycocyanin (AD5-14H12), anti-hCD303/BDCA-2 PE (AC144) from Miltenyi; anti-human CD115/M-CSFR PE (9-4D2-1E4), anti-hCD203c/E-NPP3 PE (NP4D6), anti-hCD284/TLR4 PE (HTA125), anti-hFcεRI FITC (AER-37), anti-mouse CD45 Alexa700 (30-F11) from BioLegend. The labeled cells were analyzed using FACSCantoII or FACSAria (BD Biosciences).

Morphological analysis

Cytospin specimens of FACS-purified human myeloid cells were prepared with a Shandon Cytospin 4 cytocentrifuge (Thermo Electric). To identify nuclear and cytoplasmic characteristics of each myeloid cell, cytospin specimens were stained with 100% May–Grünwald solution (Merck) for 3 min, followed by 50% May–Grünwald solution in phosphate buffer (Merck) for an additional 5 min, and then with 5% Giemsa solution (Merck) in phosphate buffer for 15 min. All staining procedures were performed at room temperature. Light microscopy was performed with a Zeiss Axiovert 200 (Carl Zeiss).

In vitro cytokine stimulation and phospho-specific flow cytometry

After 2-h preculture at 37°C in RPMI 1640 (Sigma) containing 10% FBS, recipient BM cells were incubated for 15 min in medium supplemented with 100 ng/ml recombinant human IFN-γ (rhIFN-γ; BD Biosciences), 100 ng/ml recombinant human G-CSF (rhG-CSF; PeproTech), 100 ng/ml recombinant human GM-CSF (rhGM-CSF; PeproTech) or 100 ng/ml recombinant human M-CSF (rhM-CSF; R&D Systems), fixed for 10 min at 37°C with Phosflow Lyse/Fix Buffer (BD Biosciences), permeabilized for 15 min at 4°C with 0.5× Phosflow Perm Buffer IV (BD Biosciences), and labeled using the following set of Abs: anti-human CD3 PerCP–Cy5.5 (SK7), anti-hCD14 PE (M5E2), anti-hCD15 allophycocyanin (HI98), anti-hCD33 PE–Cy7 (p67.6), anti-hCD45 V450 (HI30), anti-mouse CD45 allophycocyanin–Cy7 (30-F11), and the combination of anti-human p-STAT1 Alexa488 (4a), p-STAT3 Alexa488 (4/P-STAT3), p-STAT4 Alexa488 (38/p-Stat4), p-STAT5 Alexa488, and p-STAT6 Alexa488 (18/P-Stat6), all from BD Biosciences. Phosphorylation of STAT molecules was analyzed using FACSCantoII (BD Biosciences). Digital data were converted into a heat map using an online analysis system (Cytobank; http://www.cytobank.org/) (16).

In vivo rhG-CSF treatment of humanized NSG mice

Human CB HSC-engrafted NSG recipients at 4–6 mo posttransplantation were given rhG-CSF (PeproTech) at 300 μg/kg s.c. once a day for five consecutive days. The recipients were analyzed for the frequency of $hCD45^+CD15^+CD33^{low}$ fraction (neutrophils) and $hCD45^+CD15^{-/low}$ $CD33^+$ fraction (monocytes and DCs) before and after rhG-CSF treatment.

In vitro phagocytosis by human myeloid subsets

In vitro phagocytosis was examined using Fluoresbrite Yellow Green carboxylate microspheres (Polysciences). After single-cell preparation, recipient lung and BM cells were precultured for 2 h at 37°C in RPMI 1640 (Sigma) containing 10% FBS then incubated with fluorescent beads (particle/cell ratio = 10:1) for 1 h at 37°C or 4°C and labeled with anti-mouse CD45 allophycocyanin–Cy7, anti-human CD45 allophycocyanin and anti-hCD33 PE–Cy7 (all from BD Biosciences) for identification of fluorescent $beads^+$ $hCD45^+hCD33^+$ cells. The frequencies of observed fluorescent $beads^+$ $hCD45^+hCD33^+$ cells out of total $hCD45^+hCD33^+$ cells were determined. Fluorescent $beads^+$ $hCD45^+hCD33^+$ human lung myeloid cells were purified using FACSAria (BD Biosciences) and imaged using a laser-scanning confocal microscope (Zeiss LSM 710; Carl Zeiss). The intracellular localization of fluorescent beads was confirmed by scanning z-series sections.

TLR analysis and in vivo LPS stimulation of humanized NSG mice

Surface expression levels of TLR2 and TLR4 were analyzed by FACSCantoII. To test the LPS-induced inflammatory response, human CB

HSC-engrafted NSG recipients at 4–6 mo posttransplantation were injected i.v. with LPS at 15 μg/mouse. After LPS injection, plasma was collected from 0 to 4 h. Human cytokines IL-1β, IL-6, IL-8, IL-10, IL-12p70, and TNF were measured by cytometric bead array (BD Biosciences).

IFN-γ–induced Salmonella *killing activity by humanized mouse-derived monocytes/macrophages*

Salmonella typhimurium PhoPc strain transformed with the pKKGFP plasmid was kindly provided by J.P. Kraehenbuhl (17). *S. typhimurium* was grown shaking at 180 rpm overnight in Luria–Bertani broth supplemented with 100 μg/ml ampicillin at 37°C. BM monocytes/macrophages were purified by FACSAria (BD) based on the phenotypic characterization of lineage (CD3, CD7, CD16, CD19, CD56, CD123, CD235a)-negative, mouse CD45 and Ter119-negative, human $CD45^+CD11b^+$. Aliquots of (10^4) human monocytes/macrophages derived from humanized mouse BM were cultured on collagen type I-coated 96-well plates (BD) for 24 h in either the presence or the absence of 1000 U/ml recombinant human IFN-γ (BD). Then, cells were infected with *S. typhimurium* at multiplicity of infection (MOI) of 20 at 37°C for 2 h, and the infection was confirmed by fluorescence microscopy (Biorevo BZ-9000; Keyence). For intracellular CFU determination, cells were washed twice with PBS and lysed in 0.2% Triton X-100 in PBS for 2 min, and lysates were diluted and plated onto Luria–Bertani broth agar plates containing 100 μg/ml ampicillin for colony enumeration.

Statistical analysis

The numerical data are presented as means ± SEM unless otherwise noted. Where noted, two-tailed *t* tests were performed, and the differences with the *p* value <0.05 were deemed statistically significant (GraphPad Prism; GraphPad).

Results

Human myeloid lineage cells develop in NSG mice transplanted with human CB HSCs

Recent advances in our knowledge of innate immunity reemphasize the importance of myeloid cells for sensing, capturing, and processing Ags for the initiation of innate and acquired phases of immune responses. The development of human myeloid cells in HSC-engrafted NSG mice has not previously been studied in detail. To evaluate in vivo differentiation and function of human myeloid lineage cell populations, we transplanted 1×10^4–3×10^4 purified human $lineage^-CD34^+CD38^-$ CB HSCs intravenously into sublethally irradiated newborn NSG mice. At 4–6 mo posttransplantation, we confirmed high levels of human hematopoietic chimerism and multilineage differentiation of human immune subsets as evidenced by flow cytometry (Fig. 1A, 1B). In addition to the reconstitution of human adaptive immunity ($CD3^+$ T cells and $CD19^+$ B cells), we identified the development of human innate immune cell subsets such as $CD56^+$ NK cells and $CD33^+$ myeloid cells in the recipient mice. The frequency of human myeloid lineage cells was higher in the recipient BM (30.7 ± 3.9%, $n = 11$) compared with that in the spleen (6.2 ± 1.2%, $n = 11$, $p < 0.0001$ by paired two-tailed *t* test) and PB (7.1 ± 1.3%, $n = 11$, $p < 0.0003$) (Fig. 1B).

We then identified the subsets of human myeloid cells present in the humanized NSG recipient mice through flow cytometry. Human myeloid subsets are classified into HLA class II-negative granulocytes and class II-positive APCs. In the BM and spleen

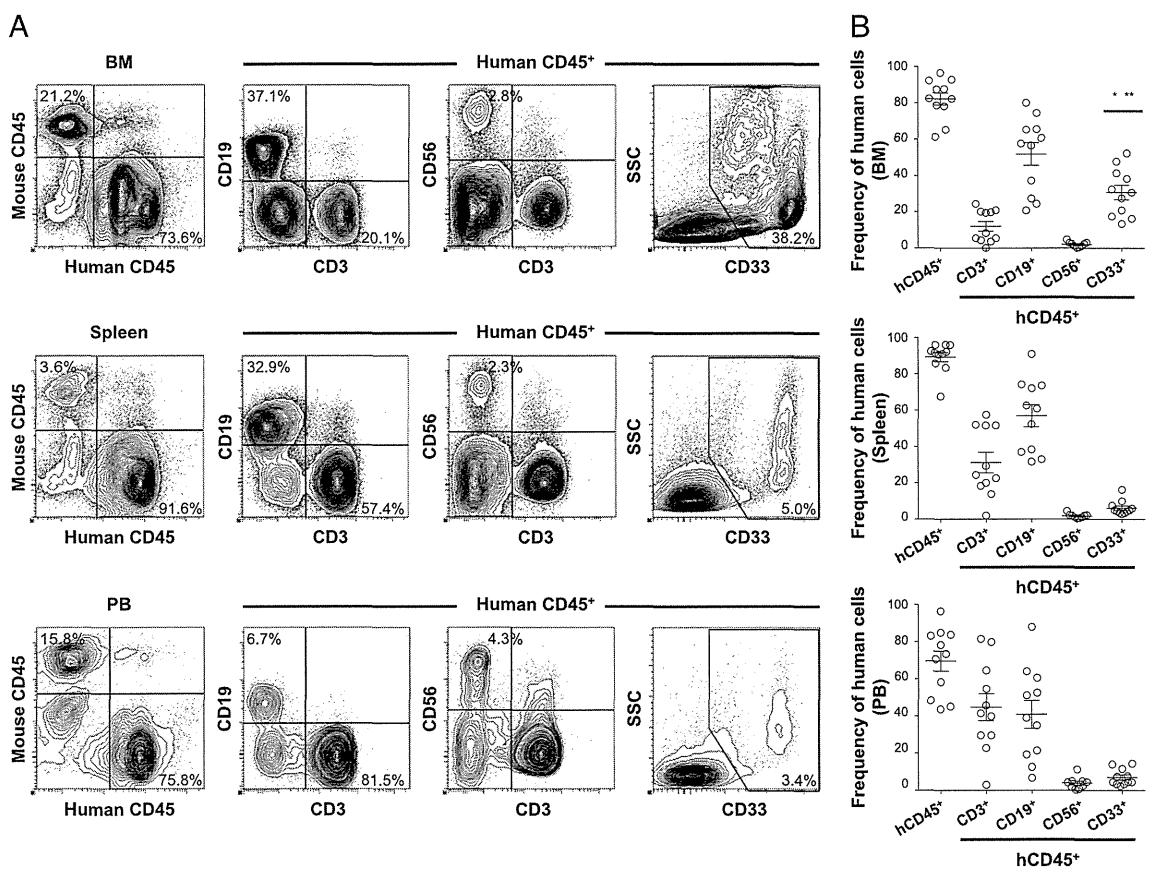

FIGURE 1. Development of human acquired and innate immunity in NSG recipients after transplantation of human CB HSCs. (**A**) Representative sets of flow cytometry contour plots demonstrating the development of human $CD45^+$ hematopoietic cells, $hCD3^+$ T cells, $hCD19^+$ B cells, $hCD56^+$ NK cells, and $hCD33^+$ myeloid cells in the BM, spleen, and PB of an NSG recipient. (**B**) Human $CD45^+$ hematopoietic chimerism and the frequencies of $hCD3^+$ T, $hCD19^+$ B, $hCD33^+$ myeloid cells ($n = 11$ each, frequency of myeloid cells in BM compared with spleen, $*p < 0.0001$, and with PB, $**p < 0.0003$) and $hCD56^+$ NK ($n = 9$ each) cells in the BM, spleen, and PB of NSG recipients at 4–6 mo posttransplantation are summarized.

of NSG recipients at 4–6 mo posttransplantation, we observed differentiation of both human granulocytes and APCs. Among the granulocyte lineage, human $CD15^+CD33^{low}HLA\text{-}DR^-$ neutrophils, $CD117^-CD123^+CD203c^+$ basophils, and $CD117^+CD203c^+HLA\text{-}DR^-$ mast cells were observed in the recipient BM and spleen. Analyses of APC populations found that $CD14^+CD33^+HLA\text{-}DR^+$

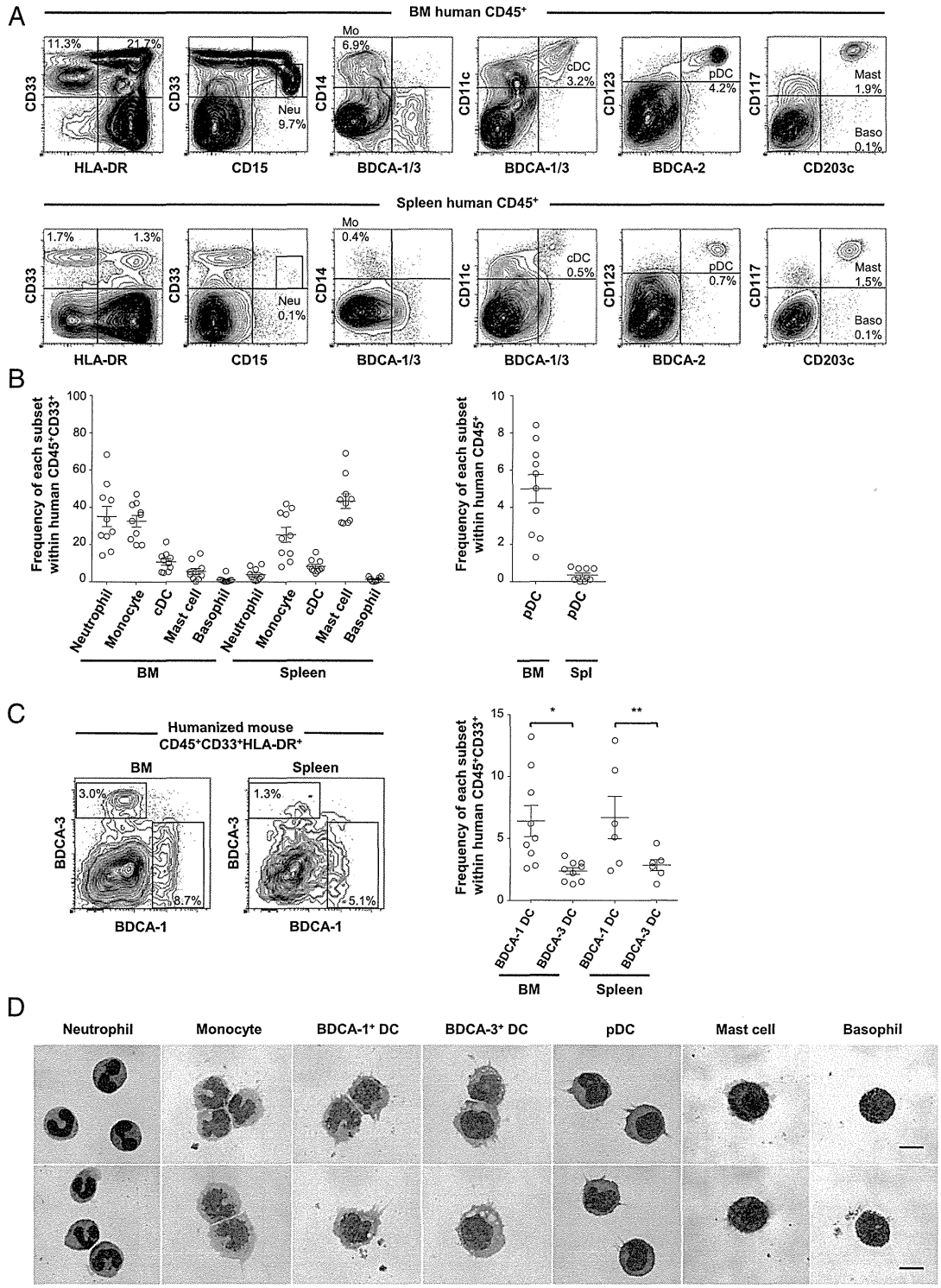

FIGURE 2. Development of human myeloid lineages in NSG recipients. (**A**) Representative flow cytometry contour plots demonstrating differentiation of human $HLA\text{-}DR^-$ granulocytes and $HLA\text{-}DR^+$ APCs in the BM and spleen of an NSG recipient. (**B**) The frequencies of human neutrophils, monocytes, cDCs, mast cells, basophils, and pDCs in the BM and spleen of NSG recipients are summarized ($n = 10$). (**C**) In the humanized mouse BM and spleen, two distinct subsets of DCs, BDCA-1^+ DCs and BDCA-3^+ DCs, were identified in $HLA\text{-}DR^+CD33^+CD11c^+$ conventional DCs. Frequencies of the two DC subsets within BM and spleen $hCD45^+CD33^+$ cells are shown (BM, $n = 9$, $^*p = 0.007$, significant differences between cDCs; spleen, $n = 6$, $^{**}p = 0.046$). (**D**) Human myeloid cells isolated by cell sorting of recipient BM demonstrate characteristic morphological features on May–Grünwald–Giemsa stain. Baso, Basophils; Mast, mast cells; Mo, monocytes; Neu, neutrophils. Scale bars, 10 μm.

BDCA-1$^-$BDCA-3$^-$ monocytes, CD14$^-$CD33$^+$HLA-DR$^+$BDCA-1$^+$ or BDCA-3$^+$ cDCs, and CD123$^+$BDCA-2$^+$HLA-DR$^+$ pDCs developed in the recipients BM and spleen (Fig. 2A, 2B). The frequency of CD15$^+$CD33^{low}HLA-DR$^-$ neutrophils within human CD45$^+$CD33$^+$ myeloid cells were present at the highest level in the BM (35.0 ± 5.4%, n = 10), whereas CD117$^+$CD203c$^+$FcεRI^{low} HLA-DR$^-$ mast cells developed at a higher efficiency in the recipient spleen (43.3 ± 4.0% within CD45$^+$CD33$^+$, n = 10) (Fig. 2B). Among human APCs developing in the NSG recipients, monocytes accounted for the highest frequency in total myeloid cells both in the BM (32.6 ± 3.1%, n = 10) and spleen (25.2 ± 4.0%, n = 10). cDCs are divided into two subsets according to the expression of BDCA-1 and BDCA-3. Within human CD45$^+$CD33$^+$ myeloid cells, the frequencies of BDCA-1$^+$ DCs accounted for 6.4 ± 1.2% in BM (n = 9) and 6.7 ± 1.7% in spleen (n = 6) and were significantly higher than those of BDCA-3$^+$ DCs (2.4 ± 0.3% and 2.8 ± 0.4%, respectively) (Fig. 2C). We then performed flow cytometric analysis using the same mAbs to determine the frequencies of each myeloid subset in primary BM MNCs. Although we could not directly compare human neutrophil development, the proportion of human monocytes, BDCA1$^+$ cDCs, BDCA3$^+$ cDCs, and pDCs was similar between primary human BM and humanized mouse BM (Supplemental Fig.1). In addition to the expression analysis of cell surface molecules, we performed May–Grünwald–Giemsa staining to identify the morphology of the myeloid lineage cells developing in the NSG recipients. Human myeloid cells purified from NSG recipient BM exhibited characteristic morphological features (Fig. 2D).

Human myeloid lineage cells developing in NSG recipients demonstrate intact functional responses to human cytokines in vitro and in vivo

We confirmed the development of various human myeloid subsets in the BM and spleen of NSG recipients and next examined the expression of human cytokine receptors including IFN-γR, G-CSFR, GM-CSFR, and M-CSFR compared with that in human CB (Fig. 3A–C). By using human CD45$^+$CD33$^+$ CB myeloid cells as control, we confirmed that human CD45$^+$CD33$^+$ cells in the recipient BM expressed comparable levels of IFN-γR, G-CSFR, GM-CSFR and M-CSFR (n = 5, no significant difference between humanized mouse BM and CB, p = 0.6444, p = 0.0985, p = 0.3879, and p = 0.5816, respectively) (Fig. 3D).

To demonstrate functional responses to human cytokine stimulation at a cellular level, we examined the phosphorylation of STAT molecules using flow cytometry. Recent studies have revealed that hematopoietic cytokine receptor signaling is largely mediated by JAK kinases and STAT molecules known as the downstream transcription factors (18). BM cells from NSG recipients (n = 3) were

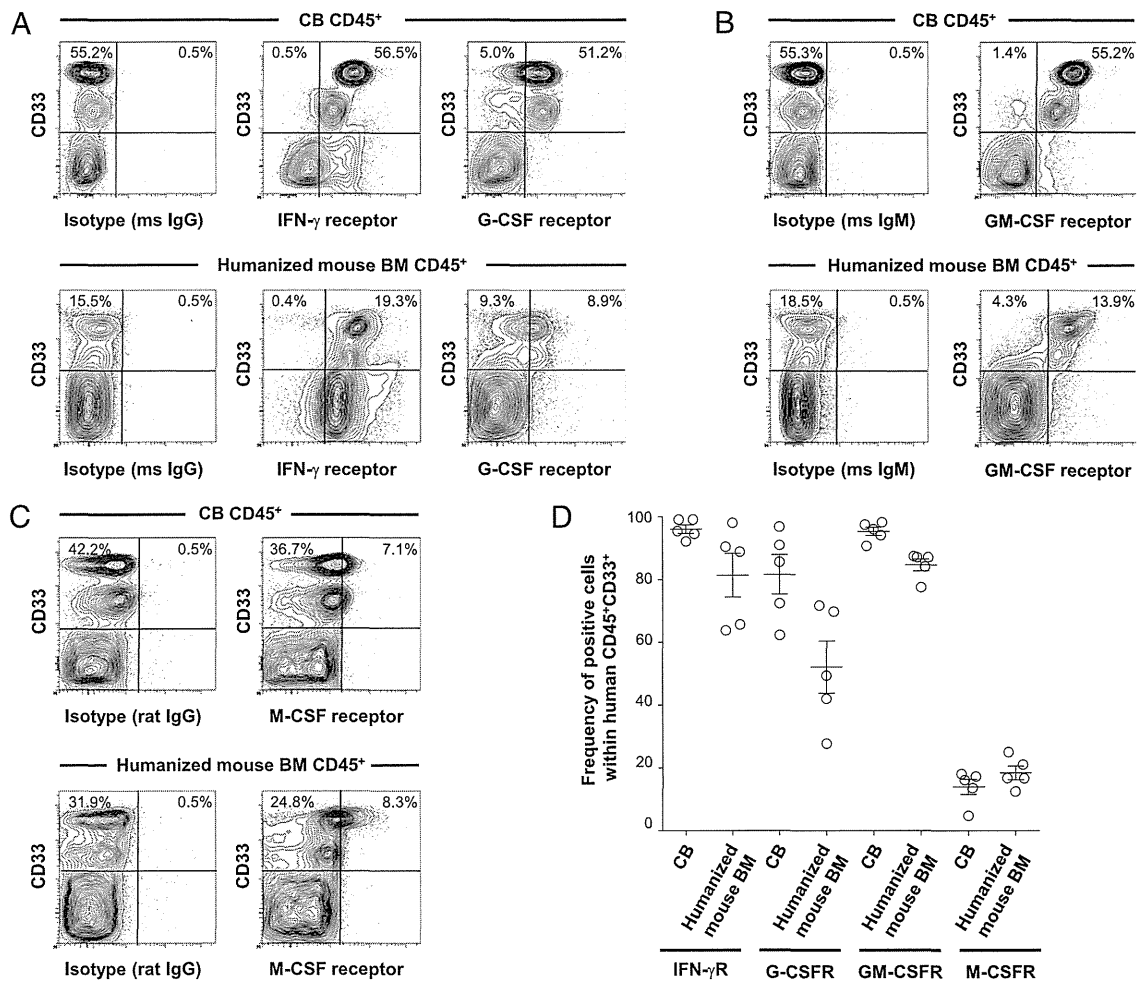

FIGURE 3. Expression of cytokine receptors on human myeloid cells in NSG recipients. (**A–C**) Representative flow cytometry contour plots demonstrating the expression of IFN-γR, G-CSFR, GM-CSFR, and M-CSFR by CB hCD45$^+$CD33$^+$ myeloid cells (top) and by hCD45$^+$CD33$^+$ myeloid cells derived from humanized NSG BM (bottom). Contour plots for isotype control Ig are also shown. (**D**) Expression of each cytokine receptor within hCD45$^+$CD33$^+$ cells is summarized (CB, n = 5; humanized NSG BM, n = 5).

stimulated with rhIFN-γ, rhG-CSF, rhGM-CSF, or rhM-CSF in vitro for 15 min at 37°C. In neutrophils and monocytes, rhGM-CSF specifically induced STAT5 phosphorylation, but not irrelevant STATs (e.g., STAT4 and STAT6) (Fig. 4A, 4C). Additionally, rhIFN-γ and rhG-CSF induced optimal STAT phosphorylation (Fig. 4B, 4D, 4E). Indeed, rhIFN-γ stimulation resulted in intracellular STAT1, STAT3, and STAT5 phosphorylation, and rhG-CSF stimulation induced STAT3 and STAT5 phosphorylation, respectively (Fig. 4E). These results indicate that intact molecular events occur in human neutrophils and monocytes in response to recombinant human cytokines in vitro.

We next investigated in vivo cytokine response by human myeloid cells in the NSG humanized mice. Stimulation with rhG-CSF in vivo is known to induce proliferation of myeloid precursors and mobilization of myeloid subsets from BM (19). After in vivo treatment of humanized mice by rhG-CSF for 5 d, the frequencies of $hCD45^+CD15^+CD33^{low}$ fraction (human neutrophils) and $hCD45^+CD15^{-/low}CD33^+$ fraction (human monocytes and DCs) increased in the PB (three out of three recipients) (Fig. 4F). These findings indicate that human myeloid cells developing in the humanized NSG recipients demonstrate functional cytokine response both in vivo and in vitro.

Human inflammatory response via TLR signaling

Along with the role of cytokine receptor signaling in development and function of myeloid cells, signaling via TLRs serves fundamental roles in evoking systemic inflammatory response by myeloid cells (20). We therefore analyzed the expression of TLRs in human myeloid cells developed in the engrafted NSG recipients by flow cytometry. We examined the surface expression of TLR2 and TLR4 in the human myeloid cells developed in the humanized mouse BM. TLR2 is specifically expressed in human monocytes and $BDCA1^+$ DCs, and TLR4 is expressed in the four distinct myeloid subsets, neutrophils, monocytes, $BDCA1^+$ cDCs, and $BDCA3^+$ cDCs (Fig. 5A, 5B). The expression of TLR4 was also confirmed in humanized mouse BM-derived monocytes and other myeloid subsets, which has led us to investigate the in vivo response of human innate immunity against LPS, a potent TLR4

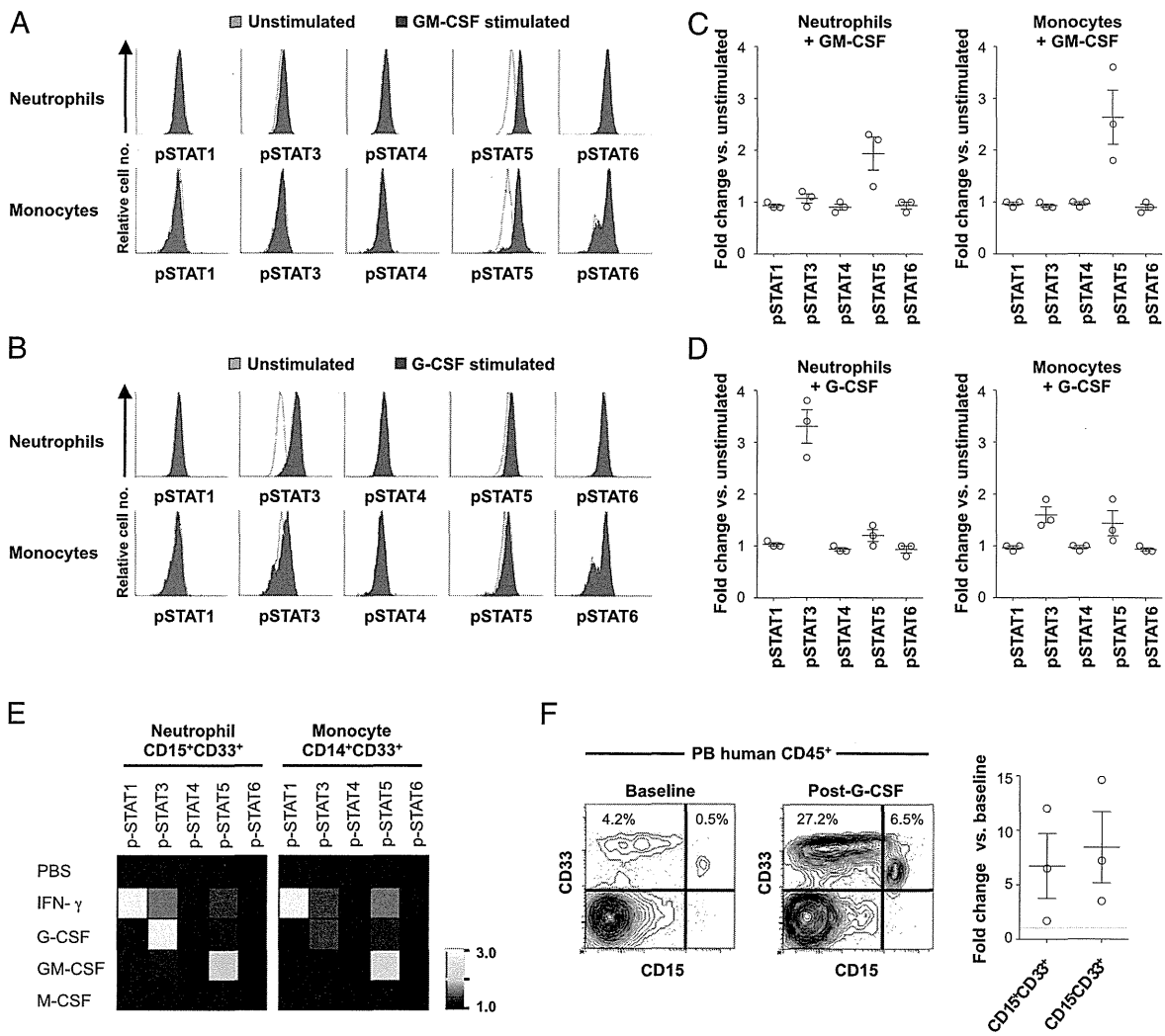

FIGURE 4. Human myeloid lineage cells developing in NSG recipients demonstrate cytokine responses in vitro and in vivo. (**A** and **B**) Phosphorylation of STAT1, STAT3, STAT4, STAT5, and STAT6 in human neutrophils and monocytes derived from an NSG recipient BM after in vitro stimulation with rhGM-CSF (A) and with rhG-CSF (B) was measured by flow cytometry. (**C** and **D**) Results from three independent experiments using three different recipients are summarized. (**E**) Heat map representation of STAT phosphorylation in human neutrophils and monocytes in an NSG recipient BM after in vitro cytokine treatment relative to PBS exposure is shown. (**F**) Representative flow cytometry contour plots demonstrating expansion of myeloid lineage cells in the PB of an NSG recipient in response to in vivo rhG-CSF administration. Frequencies of $hCD45^+CD15^+CD33^{low}$ and $hCD45^+CD15^{-/low}CD33^+$ myeloid cells were increased after in vivo rhG-CSF treatment in PB of NSG recipients for 5 d.

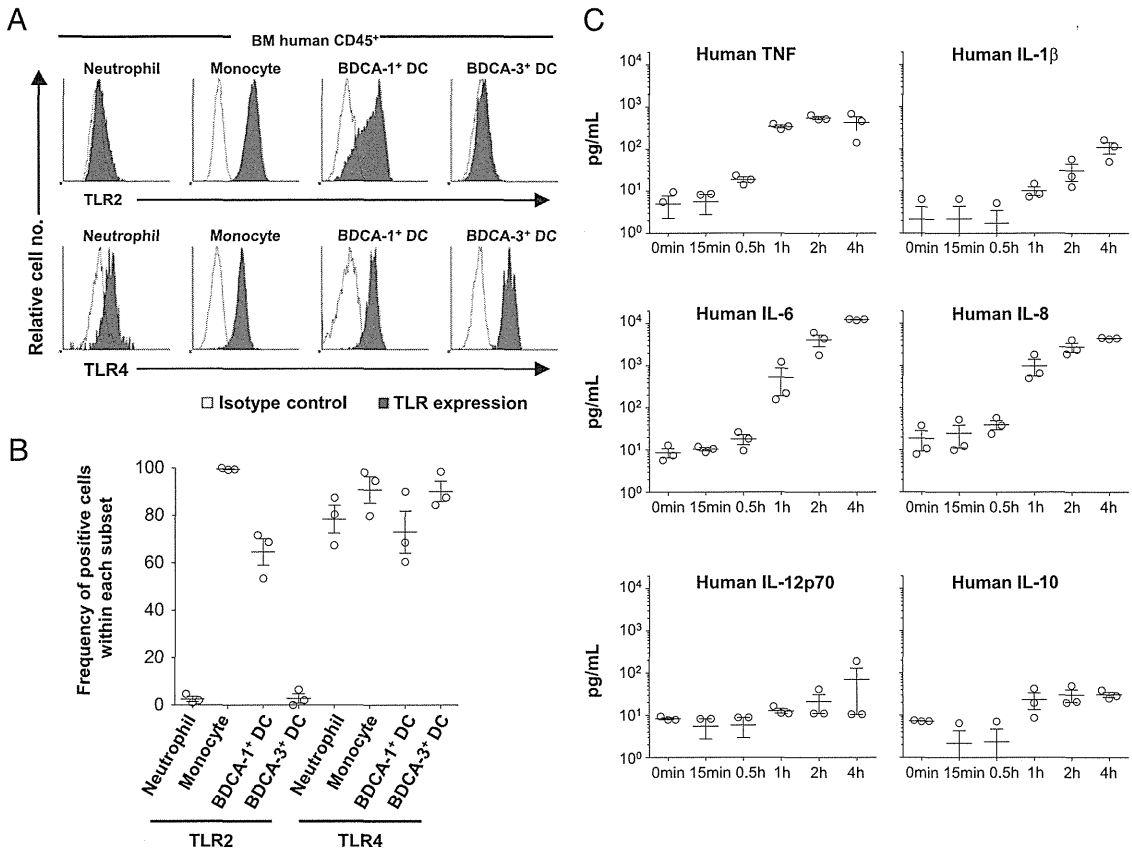

FIGURE 5. Expression of TLRs and response to TLR adjuvant by humanized mouse-derived myeloid subsets. TLR expression is analyzed in the granulocytes, monocytes, and cDCs derived from the humanized NSG recipient BM. (**A** and **B**) Expression of TLR2 and TLR4 in neutrophils, monocytes, BDCA-1$^+$ DCs, and BDCA-3$^+$ DCs was analyzed by flow cytometry. (**C**) At different time points after the injection of 15 μg LPS into humanized NSG recipients, human-specific cytokine levels in plasma were evaluated by cytometric bead array (n = 3).

ligand and endotoxin. To this end, we have administered 15 μg LPS to NSG humanized mice followed by detection of human inflammatory cytokines by flow cytometry. Bead-attached Abs for human cytokines did not detect 5000 pg/ml of mouse cytokines demonstrating that these Abs and analyses are human-specific (Supplemental Fig. 2). Of the cytokines examined, we have seen the significant elevation of plasma levels of human IL-6, human IL-8, and human TNF (Fig. 5C). Time-dependent kinetics showed that the prompt response of human innate cells to the LPS was achieved between 30 min and 1 h after injection. Consequently, humanized mice could be used to examine human innate immune response against infectious organisms and to predict inflammatory response provoked by the TLR ligands.

Human myeloid cells present in NSG recipient lung exhibit functional phagocytosis

In the human immune system, myeloid cells serve an important role in immune surveillance not only in the systemic immune compartments but also in the mucosal tissues, especially the respiratory compartment of lung protected by both mucosal and systemic immune systems (21, 22). To examine whether functional reconstruction of human myeloid cells occurs in the lung, we evaluated the differentiation and function of human myeloid lineage cells isolated from the lungs of NSG recipients. Among human CD45$^+$ cells present in the NSG recipient lung, myeloid lineage cells constituted 20.3 ± 3.8% (n = 8; a representative set of flow cytometry plots shown in Fig. 6A). The majority of human myeloid lineage cells residing in the recipient lungs were CD33$^+$ CD14$^+$HLA-DR$^+$ monocytes/macrophages (60.9 ± 5.1% within huCD45$^+$CD33$^+$, n = 8) (Fig. 6B).

The respiratory tract represents a major port of entry for inhaled pathogenic organisms, and resident alveolar monocytes/macrophages play a major role in surveillance and immune defense. To confirm the phagocytic function of human monocytes/macrophages present in the lungs of NSG recipients, we performed in vitro phagocytosis assay using yellow-green fluorescent beads by flow cytometry and confocal microscopy imaging. After in vitro incubation of NSG recipient-derived human CD45$^+$ cells with 1 and 2 μm fluorescent beads at 37°C, uptake of beads was noted in 9.0 and 7.9% of hCD45$^+$CD33$^+$ human myeloid cells, respectively (Fig. 6C). It should be noted that uptake of fluorescent beads was observed only in hCD45$^+$CD33$^+$ myeloid cells, but not in hCD45$^+$CD33$^-$ lymphoid cells (Fig. 6C). This demonstrates that the fluorescent bead uptake specifically represents phagocytotic function by human lung myeloid cells, not nonspecific uptake of the beads or binding or coating of the cells by the beads. The efficiency of uptake was 24.4 ± 3.0% in the lung-derived hCD45$^+$CD33$^+$ cells (n = 6, p = 0.001 compared with 4°C incubation by two-tailed t test), equivalent to that in BM-derived hCD45$^+$CD33$^+$ cells (16.6 ± 2.7%, n = 4, p = 0.01 compared with 4°C incubation by two-tailed t test) (Fig. 6C, 6D).

Next, phagocytosis of fluorescent beads by human myeloid cells was confirmed by direct visualization by confocal microscopy. Three-dimensional confocal imaging demonstrated intracellular localization of the fluorescent bead signal in sorted fluorescent bead (YG signal)$^+$hCD45$^+$CD33$^+$ human myeloid cells, confirming the